Sl. No.	IIT Ropar List of Recent Publications with Abstract Coverage: October, 2025
A	**Book Chapter(s)**
1.	Integrated and hybrid advanced oxidation processes S Keshri, S Sudha, **K Kumar** - Advanced Oxidation Process-Based Integrated and Hybrid Technologies for Degradation of Pharmaceuticals and Personal Care Products, Book Chapter: 2025 **Abstract:** Water is and will continue to be significant in sustainable development, yet it remains scarce. The exponential and universal demand for quality water, whether for drinking purposes, industry, sanitation, etc., will continue to rise exponentially. Both world population increase and climate change are alarming factors that cause concerns over decline in freshwater resources and availability. Pharmaceutical waste that contains active pharmaceutical ingredients has been shown to have a harmful impact on the environment because of their presence in groundwater, surface water, and even drinking water. Their low biodegradability and high hydrophilicity make it difficult to eliminate them from water using conventional methods. In this framework, along with technological advancement, including the integration of advanced oxidation processes (AOPs) and combining it with biological treatment, it is found to be effective in reducing the concentration of pharmaceutical and personal care product (PPCP) pollutants to the desired level. This chapter addresses the combination of hybrid and integrated AOPs and biological processes used in the degradation of PPCP organic pollutants in wastewater.
2.	Role of B cells, macrophages, and dendritic cells in recurrent pregnancy loss **JA Malik, JN Agrewala** - Reproductive Immunogenetics: A Molecular and Clinical Overview: Immune Cells and Immunotherapeutics in Recurrent Pregnancy Loss, Book Chapter: 2025 **Abstract:** The critical balance between immune reactivity and embryonic antigenic tolerance is essential for successful pregnancy outcomes. The maternal immune system must orchestrate a delicate immune response, allowing fetal development while protecting against infections. This balance is particularly challenging as the fetus is semiallogeneic, containing maternal and paternal antigens. Key immune cells, including dendritic cells, macrophages, B cells, NK cells, and T cells, are present at the maternal-fetal interface, where they engage in complex crosstalk with stromal cells and trophoblasts. Each cell type contributes differently to maintaining immune tolerance and protecting against pathogens during pregnancy. Recent research has shed light on the roles of B cells, macrophages, and dendritic cells in pregnancy complications such as preeclampsia, preterm birth, spontaneous abortion, infection, and intrauterine growth restriction. Imbalances in cellular immunity at the maternal-fetal interface can lead to adverse outcomes, highlighting the importance of understanding the dynamic changes in immune cell interactions during pregnancy. A deeper understanding of these immune cell dynamics is essential for the early diagnosis of pathological pregnancy and the development of potential therapeutic interventions. Future research should focus on elucidating the specific functions of B cells, macrophages, and dendritic cells in both physiological and pathological pregnancy and exploring novel ideas for interventions to restore immune balance at the maternal-fetal interface. Building upon previous investigations can pave the way for improved maternal and fetal health outcomes.
3.	Role of CD8+ cytotoxic T cells in recurrent pregnancy loss **JA Malik, JN Agrewala** - Reproductive Immunogenetics: A Molecular and Clinical Overview: Immune Cells and Immunotherapeutics in Recurrent Pregnancy Loss, Book Chapter: 2025 **Abstract:** Harnessing maternal immune adaptability is crucial for ensuring a successful pregnancy. The complexities of immune regulation can sometimes lead to pregnancy complications such as recurrent pregnancy loss (RPL). Immune dysregulation is at the core of these challenges, a complex interplay of maternal-fetal immune interactions. Throughout conception, fetal antigens encounter the maternal immune system through various avenues, from prepregnancy exposure to postpregnancy microchimerism. These encounters leave their mark on the maternal immune system, triggering CD8 T cells primed to respond to fetal antigens upon reexposure. While this process may seem risky and

	can result in RPL, evidence suggests that memory CD8 T cells often act as protectors of tolerance rather than triggers of immune reactivity. Their relationship with fetal cells highlights the delicate balance necessary for a successful pregnancy. Recent research has shed light on the role of CD8 T cells in RPL. Contrary to previous beliefs, it has been discovered that CD8 T cells may not always instigate miscarriages but can contribute to the acceptance of the fetus. Studies have shown that CD8 T cells at the maternal-fetal interface, specifically those with specificity against fetal antigens, do not necessarily cause RPL. Instead, they may be crucial in maintaining tolerance between the mother and fetus. This surprising finding challenges conventional wisdom and highlights the importance of understanding the complex mechanism of the maternal immune system in pregnancy.
4.	Role of next generation advanced wireless techniques for disaster management in smart cities P Kumar, **S Bhattacharyya**, **S Darshi** - Challenges for Smart City Infrastructure, Technologies, and Their Future: Book Chapter, 2026 **Abstract:** The evolution of smart cities, driven by 5G and B5G, enhances quality of life and sustainability but faces challenges in disaster management. This chapter explores solutions using advanced communication technologies to ensure operational continuity post-disaster. Device-to-device (D2D) communication facilitates crucial message exchange between victims and relief teams without relying on base stations. Drone-assisted D2D cooperative communication (DA-DD-CC) improves reliability by incorporating drones as relays, enabling direct, drone-assisted, or combined links. Rate-splitting multi-user cooperation by drone (RSMUCD) integrates rate-splitting multiple access (RSMA) with multi-antenna drones to mitigate interference, optimize bandwidth, and boost reliability. This framework examines multi-cluster DA-DD-CC scenarios and evaluates RSMUCD against non-orthogonal multiple access (NCSD) and network-coded cooperation (NCC) schemes using metrics like outage probability, data rate, and throughput. Findings demonstrate significantly enhanced performance for disaster management in smart cities.
B	**Conference Proceeding(s)**
5.	Accelerating temporal triangle counting and betweenness centrality on GPUs **TT Parvindersingh**, **VK Tavva**, S Banerjee, C Sur - 2025 IEEE High Performance Extreme Computing Conference (HPEC), 2025 **Abstract:** Temporal graphs have become very relevant and important in diverse and rapidly cl environments, such as in social network analysis, supply-chain management, urban planning, etc. In th we consider temporal graphs and propose GPU-based implementations of two graph algorithms th widespread use, namely, Triangle Counting and Betweenness Centrality. We show that the GPU implementations are very effective, providing significant speed-up when compared to their CPU count
6.	Accelerating the self-consistent quantum transport simulation model with advanced trained neural networks **MS Yadav, A Rawat, B Rawat** - 2025 IEEE 7th International Conference on Artificial Intelligence Circuits and Systems (AICAS), 2025 **Abstract:** As semiconductor devices continue to scale into the nanometer regime, the non-equilibrium Green's function (NEGF) formalism, coupled with Poisson's equation, remains one of the most reliable methods for quantum transport simulations. However, NEGF simulation model is known to be computationally intensive due to the repetitive matrix operations and energy integrations involved, which limits their applications in device and circuit design. In this paper, we present a machine learning (ML)-based NEGF framework that uses convolutional neural networks (CNNs), long-short-term memory (LSTM) networks, and gated recurrent unit (GRU) networks to significantly accelerate computation time. Our approach replaces the computationally expensive iterative NEGF-Poisson loop by directly predicting electrostatic potentials through the ML model. By training on labeled datasets, our framework enhances computational efficiency while maintaining high accuracy. The results show that the CNN model outperforms in training accuracy and root mean square error, with only a marginally increased computation time, even when using smaller batch sizes, compared to the LSTM and GRU models.
7.	DDoS attack detection using machine learning for UAV networks

	I Sharma, **S Agarwal**, **SS Jha** - 2025 IEEE Guwahati Subsection Conference (GCON), 2025 **Abstract:** Attacks targeting network components and devices pose a significant risk to the continuity and performance of network services. Consequently, innovative technical solutions are required to mitigate these threats and enhance the efficiency of attack detection systems. This paper introduces a Distributed Denial of Service (DDoS) attack detection algorithm specifically designed for mobile Unmanned Aerial Vehicles (UAV) networks. Leveraging a Software-Defined Networks (SDN) architecture, we propose a Machine Learning (ML) based detection module that employs a novel set of features, including flow count, speed of source IP, speed of flow entry, source IP address entropy, and destination IP address entropy, to capture both static and movement-driven traffic variations effectively. Furthermore, we derive the correlation between these features at various access points (APs). This helps establish that the attack traffic pattern remains consistent as attacker nodes move between APs. Our detection module employs three ML classifiers, Random Forest (RF), Multi-Layer Perceptron (MLP), and Support Vector Machine (SVM), and our performance evaluation under diverse traffic types (TCP, UDP, and ICMP) and attack intensities (light and heavy) demonstrates that the MLP model outperforms the other two, achieving an average accuracy of around 99%, compared to approximately 95% for state-of-the-art schemes. These results underscore the robustness of our detection framework in both static and dynamic UAV network scenarios, paving the way for developing efficient, resource-aware attack mitigation systems.
8.	Enriching pre-training using fuzzy logic V Gupta, V Bharti, **A Kumar**, A Sharma, SK Singh - 2025 IEEE International Conference on Fuzzy Systems (FUZZ), 2025 **Abstract:** Graph representation learning advances graph machine learning by encoding structural and relational information into feature vectors. This study introduces a fuzzy logic-based pre-processing layer that enhances node representations by adding semantic diversity and contextual understanding. The layer models uncertainty and captures abstract semantic characteristics in graph data, addressing the limitations of conventional methods that depend solely on structural attributes. By applying defuzzification, the layer refines embeddings, improving their robustness and effectiveness for a wide range of downstream tasks. To test its robustness, we introduce Gaussian noise ranging from 2% to 10% into the datasets, simulating real-world data imperfections. We evaluate the proposed layer on GraphMamba architecture, using DeepWalk and Node2Vec as baseline node feature generation algorithms. The results show consistent improvements in accuracy, F1 scores, precision, and recall across different noise levels. Our findings demonstrate the layer's ability to preserve high representational quality, speed up convergence, and handle noisy representations effectively.
9.	GroMo25: ACM multimedia 2025 grand challenge for plant growth modeling with multiview images **S Bansal, R Bhatt, A Chander, R Kaur, M Singh**, M Kankanhalli, A El Saddik, **M Saini** - Proceedings of the 33rd ACM International Conference on Multimedia, 2025 **Abstract:** Understanding plant growth dynamics is a critical component of modern agricultural research, with applications in yield prediction, phenotyping, and sustainable crop management. Despite recent advances in computer vision and deep learning, progress in plant growth modeling has been constrained by the lack of publicly available, high-resolution, multiview, and temporally rich datasets. To address this gap, we introduce Growth Modelling **GroMo25**, the first international challenge on *plant growth modeling using multiview imagery*. In this challenge, we propose a dataset that comprises high-resolution images of four crops: wheat, mustard, radish, and okra, captured at consistent time intervals from multiple camera viewpoints under controlled environmental conditions. The challenge focuses on two key tasks: (1) *plant age prediction* and (2) *leaf count estimation*, both requiring models to use spatial and temporal plant features. GroMo25 attracted participation from multiple teams worldwide, encouraging benchmarking and innovation in vision-based plant phenotyping. The GitHub repository is publicly available at https://github.com/mriglab/GroMo-Plant-Growth-Modeling-with-Multiview-Images.

	
10.	Harnessing imperfection: Deep learning-based receiver for non-coherent distributed transmission **A Ahmad, S Agarwal, S Kaur, SS Jha**… - IEEE Transactions on Green Communications and Networking Published, 2025 **Abstract:** This paper investigates the feasibility of distributed multi-transmission in non-coherent systems using deep learning (DL), a concept we term non-coherent distributed transmission (NCDT). In this approach, multiple transmitters non-coherently send the same content to a receiver. We leverage DL to learn and capture the complex patterns arising from signal combinations with frequency and phase offsets. By engineering relevant features and designing a deep neural network with an adaptable auto-tuning mechanism, we enable precise mapping of received signals to transmitted symbols within the NCDT framework. Additionally, we develop a likelihood ratio test (LRT)-based detector as a baseline for comparison. Our simulations and experiments demonstrate that the proposed DL-based receiver achieves lower bit error rates (BER) than the other state-of-the-art DL-based and LRT-based detectors while eliminating the need for synchronization, channel state information (CSI) estimation, or precoding. Experimental validation using software-defined radios corroborates our simulation results, confirming that NCDT can be practically integrated into wireless systems without requiring hardware modifications. Notably, our results show that the proposed method achieves comparable BER performance at nearly half the transmission power, corresponding to an approximate 3 dB gain.
11.	Identification of skills for entrepreneurial thinking using natural language processing: An exploration of entrepreneurs, faculties members and design students **K Sandhu**, P Sarkar, K Subburaj - International Conference on Research into Design, 2025 **Abstract:** Identification of skills are very important in every field of study for any kind of output. Educators in engineering design education identified students skills to think as design thinkers and creative thinkers. However, no research is available on identifying the skills of Entrepreneurial Thinking. In this twenty-first century, entrepreneurial thinking is essential to learn and its helps students to solve the grand challenges on earth. Therefore, the present study's objective is to identify entrepreneurial thinking skills; the semi-structured interviews were conducted with entrepreneurs and faculty members from academia (11) with backgrounds in design, engineering, business, and ergonomics. Natural language processing is used to identify common keywords using extract keywords with term frequency-inverse documents, yet another keyword extractor, rapid automatic keywords extraction, and topic modeling with latent semantic indexing techniques. Also, brainstorming sessions were held with design students to understand their minds and their thoughts about the skills required for entrepreneurial thinking. Lastly, the Euclidean distance matrix was used to compare identified skills (Faculty members/entrepreneurs) with design students (skills that come from their minds). The overall common skills of design students and faculty members and entrepreneurs are thinking, solution, leadership, and research with zero Euclidean distance. From this results, it has been found that the faculty members/entrepreneurs have the same understanding of the skills of entrepreneurial thinking, but design students have vague knowledge of entrepreneurial thinking skill set.
12.	IoT-driven GSR stress detection: Clinical, physical, and linguistic innovations S Azim, R Kumar…**RK Singh** - 2025 Third International Conference on Networks, Multimedia and Information Technology (NMITCON), 2025 **Abstract:** This study presents a multidisciplinary framework for advancing stress detection by integrating Internet of Things (IoT) capabilities with Galvanic Skin Response (GSR) technology.

	Leveraging IoT for real-time data acquisition and analysis, we enhance GSR sensor functionality. Contributions from clinical psychology focus on elderly populations, providing insights into age-specific stress indicators and mental health correlations. Physics principles optimise sensor accuracy and data fidelity, while computer science provides the framework for data processing, machine learning models, and IoT infrastructure. The linguistic analysis supports psychologists' recommendations, confirming that GSR readings are best when communication stabilises with subjects. This interdisciplinary approach aims to develop a comprehensive system for effective stress monitoring and mangement. Our results demonstrate that advanced machine learning models, notably the Random Forest model, achieve high predictive performance in analysing stress levels from GSR data. The confusion matrix and classification report validate its efficiency in accurately distinguishing different stress levels. Feature importance analysis reveals that the GSR Stress Value is the dominant predictor, contributing approximately 90 % to stress classification, with age having a minor influence of around ∼10%. Gender and state contribute negligibly to stress classification. However, a strong positive relationship between GSR and stress levels is confirmed by a correlation analysis with a coefficient of 0.93. Gender-based differences were minimal, though females exhibited slightly higher stress levels in extreme cases, while younger individuals showed greater fluctuations in stress variability. The findings confirm that GSR data is highly reliable for identifying stress levels and analyzing workplace stressors, offering a datadriven approach to stress analysis and management with significant implications for mental health research and wellbeing strategies.
13.	MAVEN: Multi-modal attention for valence-arousal emotion network **V Ahire, K Shah, M Khan, N Pakhale, LR Sookha, M.A. Goanaie**… - Proceedings of the IEEE/CVF Conference on Computer Vision and Pattern Recognition (CVPR) Workshops, 2025 **Abstract:** Dynamic emotion recognition in the wild remains challenging due to the transient nature of emotional expressions and temporal misalignment of multi-modal cues. Traditional approaches predict valence and arousal and often overlook the inherent correlation between these two dimensions. The proposed Multi-modal Attention for Valence-Arousal Emotion Network (MAVEN) integrates visual, audio, and textual modalities through a bi-directional cross-modal attention mechanism. MAVEN uses modality-specific encoders to extract features from synchronized video frames, audio segments, and transcripts, predicting emotions in polar coordinates following Russell's circumplex model. The evaluation of the Aff-Wild2 dataset using MAVEN achieved a concordance correlation coefficient (CCC) of 0.3061, surpassing the ResNet-50 baseline model with a CCC of 0.22. The multistage architecture captures the subtle and transient nature of emotional expressions in conversational videos and improves emotion recognition in real-world situations.
14.	Numerical study on effect of variation in thickness of expanded polystyrene core in sandwich panel under axial load **HK Kassa, P Haldar**, A Ahmad - Proceedings of the 18th East Asia-Pacific Conference on Structural Engineering and Construction, Volume 3. (EASEC 2024), 2025 **Abstract:** This study examines how variations in the thickness of the Expanded Poly-Styrene (EPS) core within sandwich panels influence the axial load-carrying capacity of Precast Concrete Sandwich Panels (PCSP), which are used as infill walls in building structures. A Finite Element Analysis (FEA) approach is used to simulate the behaviour of PCSP by incorporating material properties, boundary conditions, and geometric configurations to accurately represent the behaviour of the sandwich panel based on experimental observation. Parametric studies were performed to evaluate the effects of different EPS core thicknesses specifically 60 mm, 80 mm, and 100 mm on out-of-plane displacement and axial load-carrying capacity. The result shows that the variation in EPS core thickness has no significant effect on out-of-plane displacement and the load-carrying capacity of the PCSP. This study enhances sustainable building practices by deepening the understanding of the factors that affect the performance of sandwich panels with an EPS core. Additionally, it facilitates the construction of more efficient infill walls designed for regions susceptible to seismic loads.

15.	Pureformer: Transformer-based image denoising A Gautam, A Pawar… **SK Vipparthi** - Proceedings of the IEEE/CVF Conference on Computer Vision and Pattern Recognition (CVPR) Workshops, 2025 **Abstract**: Image denoising is a crucial task in computer vision with applications in real-world smartphones image processing, remote sensing, and photography. Traditional convolution neural networks (CNNs) often struggle to reduce noise while preserving fine details due to their limited receptive fields. Transformer-based approaches, such as Restormer, improve long-range feature modeling, while PromptIR enhances local feature refinement. However, existing methods still face challenges in effectively integrating multi-scale features for robust noise reduction. We propose Pureformer, a Transformer-based encoder-decoder architecture specifically designed for image denoising. The model employs a four-level encoder-decoder structure, where each stage utilizes Multi-Dconv Head Transposed Attention (MDTA) and Gated-Dconv Feed-Forward Network (GDFN) to extract and refine multi-scale features. We proposed a feature enhancer block in the latent space expands the receptive field using a spatial filter bank, improving feature fusion and texture restoration. Skip connections between the encoder and decoder help retain spatial information, ensuring high-fidelity reconstruction. Pureformer is evaluated on the NTIRE 2025 Image Denoising Challenge dataset, achieving a test PSNR of 29.64 dB and SSIM of 0.8601. We also validated our Pureformer on existing benchmark datasets BSD68 and Urban100 datasets. The results demonstrate that Pureformer surpasses existing methods in both noise reduction and detail preservation, making it a strong choice for real-world image denoising. Access our codes and models from https://github.com/Chapstick53/NTIRE2025_cipher_vision.
16.	SegMAgNet: A comparative study of segmentation models for defect detection in additively manufactured mg alloys **A Prata**p, N Sharma, T Wu, P Karthikeyan, **N Sardana**, PA Hsiung - IEEE International Conference on Advanced Visual and Signal-Based Systems (AVSS), 2025 **Abstract:** Magnesium (Mg) alloys are increasingly used in biomedical applications due to their biodegradability, biocompatibility, and mechanical compatibility with human bone. However, fabricating these alloys using additive manufacturing techniques like Selective Laser Melting (SLM) is challenging due to their high reactivity and the potential for internal defects such as gas porosity and lack of fusion. This study presents a comprehensive evaluation of deep learning-based image segmentation methods for detecting such defects in Mg-based alloys fabricated via SLM at 80 W laser power and 500 mm/s scanning speed. X-ray Computed Tomography (XCT) was used to scan the printed samples, and 83 non-identically distributed image slices were selected to ensure variation in defect morphology. Two types of annotations—manual (using LabelImg) and threshold-based (using ImageJ)—were used to prepare datasets. These datasets were analyzed using two models: a custom U-Net with five-fold cross-validation and a U-Net with ResNet-50 backbone enhanced by patchify augmentation. The threshold-based dataset combined with U-Net + ResNet50 achieved the highest segmentation accuracy with an IoU of 86%, outperforming manual annotation-based training. This study emphasizes the importance of annotation strategy and model selection in defect detection workflows for reactive metal additive manufacturing.

17.	Smart cities' clean air: Federated bidirectional long short-term memory for enhanced air quality index forecasting **S Dey** - International Conference on Network Security and Blockchain Technology, 2025 **Abstract:** The Internet of Things (IoT) has become popular across various applications. Still, it can also contribute to air pollution through increased energy consumption, electronic waste, and emissions from manufacturing and data centers. Enhanced logistics and traffic management can lead to more vehicle use, worsening urban air quality. This paper introduces a novel approach for predicting air quality in smart cities using the Fed-BiLSTM model, which stands for Federated Bidirectional Long Short-Term Memory. As urban areas adopt IoT technologies, accurate air quality monitoring and forecasting are essential for addressing environmental challenges. The proposed *Fed-BiLSTM* model leverages federated learning for secure, decentralized training across diverse data sources, ensuring privacy while enhancing prediction accuracy. Experimental results indicate a notable enhancement in the accuracy of AQI predictions—approximately 35%, 7%, and 10% better than traditional SVR, RFERF (ML models), and RNN (DL model) approaches, respectively. This work supports efforts to create sustainable urban environments by enabling informed decision-making through reliable air quality forecasts. 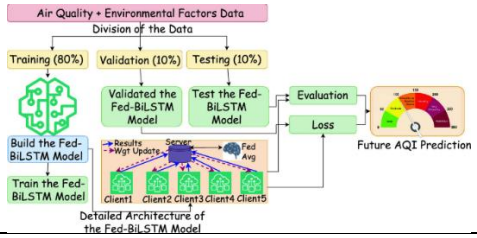
18.	TATVA: Turmeric adulteration detection using thermal video analysis **R Kaur**, **SA Khanday**… **M Saini** - Proceedings of the 1st International Workshop on Multi-modal Food Computing, 2025 **Abstract:** In this study, a novel, non-invasive, and automated approach for turmeric (Curcuma Longa L.) adulteration detection using thermal video analysis (TATVANet) is presented. A custom dataset TATVA, comprising 1,478 thermal videos of pure and adulterated turmeric, is developed under controlled laboratory conditions. Adulterated samples are prepared by introducing varying concentrations of common adulterants like starch, chickpea flour, lead chromate, and metanil yellow into pure turmeric. The primary objective of this study is to perform binary classification of turmeric samples as pure or adulterated. Thermal videos are recorded using a Fluke TiX580 thermal camera and subsequently preprocessed to extract meaningful spatio-temporal features required to train transformer-based video models. The proposed method uses the thermal signature of turmeric in conjunction with an attention mechanism of transformer architecture. TATVANet detects the pixel intensity transition between thermal video frames over time, capturing the heat conduction dynamics. TATVANet incorporates patch embedding, substantial down sampling, VIT encoder layer, and CLS recalibration. The proposed method achieves an accuracy of 92.90% with an average precision of 0.94 and outperforms state-of-the-art approaches that mostly analyze RGB and thermal images.
19.	The illusion of unlearning: The unstable nature of machine unlearning in text-to-image diffusion models N George, **KN Dasaraju**, RR Chittepu, KR Mopuri - Proceedings of the Computer Vision and Pattern Recognition (CVPR), 2025 **Abstract:** Text-to-image models such as Stable Diffusion, DALL•E, and Midjourney have gained immense popularity lately. However, they are trained on vast amounts of data that may include private, explicit, or copyrighted material used without permission, raising serious legal and ethical concerns. In light of the recent regulations aimed at protecting individual data privacy, there has been a surge in Machine Unlearning methods designed to remove specific concepts from these models. However, we identify a critical flaw in these unlearning techniques: unlearned concepts will revive when the models are fine-tuned, even with general or unrelated prompts. In this paper, for the first time, through an extensive study, we demonstrate the unstable nature of existing unlearning methods

	in text-to-image diffusion models. We introduce a framework that includes a couple of measures for analyzing the stability of existing unlearning methods. Further, the paper offers preliminary insights into the plausible explanation for the instability of the mapping-based unlearning methods that can guide future research toward more robust unlearning techniques. Codes [1] for implementing the proposed framework are provided.
20.	Understanding user experience: Exploration of various definitions using natural language process S Kaur, K Sandhu, **P Sarkar**… - International Conference on Research into Design, 2025 **Abstract:** Understanding the experience of products and users are critical aspect in design science. In daily life, individuals interact with various physical or digital interfaces. However, the concept of User Experience (UX) often remains ambiguous for designers, who struggle to differentiate between empathy, usability, and interaction. This study aims to clarify the definition of UX by identifying key features related to outcome, novelty, and value across multiple existing definitions. Sixteen commonly cited definitions of UX were analyzed using natural language processing (NLP) with cosine similarity to determine the prevalence of specific features. These definitions were selected based on the frequency of three feature categories: outcome (observable, satisfaction, emotion, and engagement), novelty (uniqueness, freshness, innovation, and adaptability), and value (task efficiency, task effectiveness, ethics, and accessibility). For the outcome-related features, the cosine similarity for "observable" was 0.24 (Definition 6), "satisfaction" was 0.47 (Definition 9), "emotion" was 0.32 (Definition 15), and "engagement" was 0.38 (Definition 12). In terms of novelty, the cosine similarity for "uniqueness" was 0.25 (Definition 6), "freshness" was 0.34 (Definition 9), "innovation" was 0.41 (Definition 9), and "adaptability" was 0.38 (Definition 12). Regarding value features, the cosine similarity for "task efficiency" was 0.48 (Definition 12), "task effectiveness" was 0.42 (Definition 12), "ethics" was 0.28 (Definition 6), and "accessibility" was 0.39 (Definition 9). Following this analysis, a brainstorming session was conducted with design students (n = 5) to gather their perspectives on these definitions and compare them to a newly developed UX definition. The results suggest that design students had an unclear understanding of UX and its core meaning in the context of product design.
21.	Urban resilience: Using autoencoder-decoder LSTM model with green roofs and vertical gardens to combat air pollution **S Dey** - International Conference on Network Security and Blockchain Technology, 2025 **Abstract:** Amid rising urbanization and environmental challenges, sustainable solutions are increasingly vital. This paper examines the role of **green roofs** and **vertical gardens** in enhancing urban resilience by reducing air pollution. By integrating these green infrastructures with the **Autoencoder-Decoder-based Long Short-Term Memory (AeD-LSTM)** model, cities can significantly lower pollution levels and improve air quality, promoting healthier living environments. The research quantifies the pollution reduction potential of these green strategies, showing significant decreases in pollution levels post-implementation. It also highlights the synergistic advantages of combining green roofs and vertical gardens, contributing to more resilient urban ecosystems. The findings offer important insights for urban planners and policymakers advocating for green infrastructure to improve urban resilience and sustainability. The proposed model achieves 30 and 40% better accuracy in terms of R2 -score and custom accuracy metrics, respectively. Also, this paper demonstrates a 30% energy savings using the energy consumption metric from the multi-LSTM autoencoder model.
C	**Article(s)**

22.	[7] Helicene-backboned quaternary ammonium salts: Synthesis, photophysical investigation, and lysosomal tracking **Deepshikha, AC Shaikh, SS Bisht, N Lal, P SINGH, JA Malik, J Agrewala** - Journal of Materials Chemistry B, 2025 **Abstract:** Polyaromatic quaternary ammonium salts (PQASs) are of significant interest due to their promising applications in biological and materials sciences. The incorporation of a heteroatom significantly modifies the electronic and chemical properties of these molecules, influencing their absorption and emission characteristics, as well as the HOMO–LUMO gap. Herein, we report the synthesis and photophysical investigation of [7]helicene-backboned quaternary ammonium salts. These compounds exhibit excellent stability, absorb light in the visible region with λ_{abs} ranging from 385 to 395 nm, and show emission in the green wavelength spectrum at λ_{em} between 541 and 552 nm. Also, they are redox-active and feature a structurally defined double helical axis. Single-crystal X-ray diffractometry has demonstrated the presence of a double helical structure within the crystal packing, which is characterized by the linkage of M–P and P–M heterodimers. Additionally, they show photoluminescence capability (ϕ_f) of up to 0.57, with fluorescence lifetimes in the range of 1.81–3.17 ns. Notably, these fluorophores turned out to be potential cell imaging agents. Colocalization studies that utilized LysoTracker Red probes as standard lysosomal trackers demonstrated that the [7]helicene QAS probe is efficacious in specifically labeling lysosomes in the neuroblastoma (N2a) cell line and RAW 264.7 macrophage cells. Additionally, to elucidate their electronic profiles, we employed time-dependent density functional theory calculations.
23.	A comparative analysis of periodic advertisements and connections in Bluetooth low energy **S Gautam, S Kumar, PP Singh** - IEEE Wireless Communications Letters, 2025 **Abstract:** Bluetooth Low Energy (BLE) periodic advertisements and connections share core protocol mechanisms—synchronized secondary advertising channels, fixed transmission intervals, and channel hopping—despite the former being connectionless. We present the first empirical study directly comparing these two modes for unidirectional data transfer in a single transmitter–receiver setup. Empirical measurements across varying data sizes and transmission intervals show that, even for large 244-byte data, periodic advertisements with two application-layer retransmissions use up to 33% and 62% less energy than connections (even with peripheral latency) at long intervals (80 s) on LE 1M and 2M PHYs, respectively, while maintaining similar data transfer reliability. These findings highlight a previously underexplored potential of periodic advertisements as a compelling alternative for energy-constrained, unidirectional deployments requiring infrequent transfers.
24.	A generalized modular battery pack topology with active cell balancing technique **A Ahmad, AVR Teja, S Payami** - IEEE Transactions on Industrial Electronics, 2025 **Abstract:** This article presents a novel generalized modular battery pack with any “n” parallel battery strings of any “m” series connected cells where ((m, n) ∈Z+). This novel battery pack prevents circulating current and also balances the entire battery pack using the proposed boost-based active cell balancing strategy. The proposed cell balancing topology employs only two active switches per cell and utilizes “n” inductors for a m × n cell battery pack, allowing efficient active balance throughout the pack. A detailed theoretical analysis is presented, and operating conditions are systematically derived to maximize output power and achieve optimal efficiency. The proposed topology and balancing technique are also simulated using MATLAB/Simulink for a three parallel strings of three series connected cells battery pack and the results are presented. These results are also experimentally verified using BAKH18650CIL battery cells in the laboratory. It could achieve cell balance while operating at 95.92% efficiency.

25.	A geometric semantic model and parts-of-sense inference annotation framework K Pala, **S Shalu**, V Nedumpozhimana, **KK Choudhary** - Frontiers in Artificial Intelligence, 2025 **Abstract:** We introduce a geometric semantic model designed to capture fine-grained semantic representations in a multidimensional space. Building on this model, we develop a novel annotation framework that facilitates detailed semantic analysis across languages. Central to our approach is a set of Parts-of-Sense Inference (POSI) tags: 135 interpretable four-letter codes that annotate subtle semantic attributes often overlooked by traditional models. To evaluate the cross-linguistic and cross-structural applicability of this framework, we annotate expressions in four typologically diverse languages. Our results demonstrate that the proposed model provides an interpretable, cognitively plausible approach to semantic representation and can serve as a robust tool for investigating language processing and meaning inference across linguistic contexts.
26.	α- induced neutron emission from 27 : A cross-section study **R Roy**, DA Testov…**M Kaur**, A Kuşoğlu… **S Singh**… - Physical Review C, 2025 **Abstract:** Aiming for a better understanding of the 27Al(α,n)30P reaction, new cross-section measurements for this reaction have been carried out using 27Al targets of thicknesses 20 μg/cm2 and 63 μg/cm2 for α-energy range of 2.5–5.2 MeV and 3.4–5.2 MeV, respectively. An array of twenty-eight 3He counters, providing high and almost flat neutron-detection efficiency up to about 3 MeV neutron energy, has been used for the experiment. The amount of 13C contamination in the 27Al target and its effect on the measured total neutron cross sections has also been reported. The measured cross sections have been interpreted using the dynamical cluster-decay model and the compound Hauser-Feshbach model. 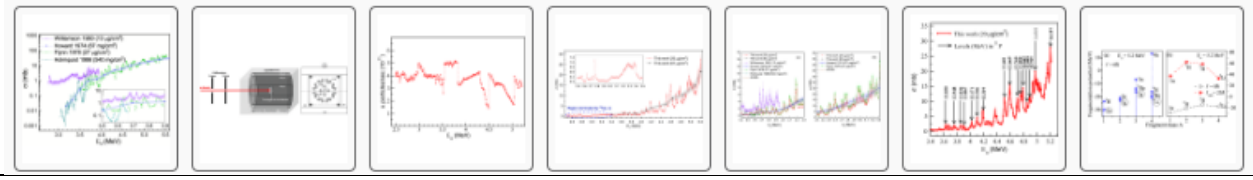
27.	A neural network guided approach for repeater optimization in multilayer graphene on-chip interconnect networks including TSVs AK Jakhar**, R Sharma**, A Dasgupta, S Roy - IEEE Journal on Multiscale and Multiphysics Computational Techniques, 2025 **Abstract:** In this paper, an artificial neural network (ANN) guided approach is developed for the repeater optimization in multilayer graphene on-chip interconnect networks. The key attribute of the proposed approach is the use of two distinct ANNs to generalize the target objective functions of interconnect networks in terms of (i) the geometrical parameters of the vertical through silicon vias (TSVs) present in the network, and (ii) the design parameters of the fin-shaped field effect transistors (FinFETs) making up the repeaters. The first ANN (ANN1) ensures that for any change in the TSV geometry, the objective functions of the network can be accurately approximated by analytical expressions without the need for laborious SPICE simulations. The second ANN (ANN2) identifies additional tuning parameters of the repeaters besides simply the number and size of the repeaters, leading to better optimization results of the network performance. This enables performing efficient repeater optimizations in the presence of design variability of the TSVs. The generalized target objective functions of the network are then maximized/minimized using a particle swarm optimizer. Multiple numerical examples are presented in the paper to test and validate the proposed ANN guided approach.
28.	A simple and robust mesh refinement implementation in abaqus for phase field modelling of brittle fracture. **A Pandey, S Kumar** - Computer Modeling in Engineering and Sciences (CMES), 2025 **Abstract:** The phase field model can coherently address the relatively complex fracture phenomenon, such as crack nucleation, branching, deflection, etc. The model has been extensively implemented in the finite element package Abaqus to solve brittle fracture problems in recent studies. However, accurate numerical analysis typically requires fine meshes to model the evolving crack path

	effectively. A broad region must be discretized without prior knowledge of the crack path, further augmenting the computational expenses. In this proposed work, we present an automated framework utilizing a posteriori error-indicator (MISESERI) to demarcate and sufficiently refine the mesh along the anticipated crack path. This eliminates the need for manual mesh refinement based on previous experimental/computational results or heuristic judgment. The proposed Python-based framework integrates the preanalysis, sufficient mesh refinement, and subsequent phase-field model-based numerical analysis with user-defined subroutines in a single streamlined pass. The novelty of the proposed work lies in integrating Abaqus's native error estimation and mesh refinement capability, tailored explicitly for phase-field simulations. The proposed methodology aims to reduce the computational resource requirement, thereby enhancing the efficiency of the phase-field simulations while preserving the solution accuracy, making the framework particularly advantageous for complex fracture problems where the computational/experimental results are limited or unavailable. Several benchmark numerical problems are solved to showcase the effectiveness and accuracy of the proposed approach. The numerical examples present the proposed approach's efficacy in the case of a complex mixed-mode fracture problem. The results show significant reductions in computational resources compared to traditional phase-field methods, which is promising. Copyright.
29.	A target responsive benzimidazole-based self-assembled micellar system embedded smart hydrogel: an integrated approach for quantification and removal of phenylbutazone R Sharma, S Kalra, N Kaur, **N Singh** - Journal of Materials Chemistry B, 2025 **Abstract:** The unregulated use and improper disposal of active pharmaceutical ingredients (APIs), particularly phenylbutazone (PBZ), are contaminating water resources and posing serious risks to the food chain. PBZ is a nonsteroidal anti-inflammatory drug (NSAID) commonly used for treating pain and fever in animals, and its persistence in the environment due to inadequate waste management has become a cause of concern. To address this, we report the fabrication of benzimidazole-based self-assembled nanomicelles (R2 NMs) for selective detection and removal of PBZ. The successful fabrication of self-assembled R2 NMs was validated using various analytical techniques. Furthermore, the binding ability of R2 NMs was evaluated using spectroscopic and electrochemical techniques. They demonstrated a selective response toward PBZ with a response time of just 20 s and a positive cooperativity of 1.92. For on-site detection and removal of PBZ, R2 NMs were integrated into a biopolymer gel composed of starch-polyvinyl alcohol-glycerol (SPG). This system can potentially serve as a portable, smart analyte-responsive nanomicellar hydrogel (SAN hydrogel) that specifically targets and removes PBZ from contaminated water. The SAN hydrogel exhibited enhanced swelling, reduced porosity, and improved water retention. Furthermore, the removal efficiency of PBZ was assessed using the SAN hydrogel, following pseudo-first-order kinetics, with noticeable fluorescence changes occurring after various time intervals. Moreover, the PBZ removal was validated by the fluorescence switching ON-OFF mechanism, enabling real-time onsite detection of PBZ. Thus, these findings suggest that the proposed material could be effectively utilized for the on-site quantification and removal of PBZ from contaminated water.
30.	An on-body RecCoil array harvester system for extended wireless charging of misaligned quadcopters **S Jain**, IJG Zuazola, **A Sharma** - IEEE Access, 2025 **Abstract:** In conventional unmanned aerial vehicle (UAV) wireless charging systems, the quadcopter must be perfectly aligned with the charging pad to ensure effective magnetic coupling for charging. To enhance quadcopter landing flexibility, the authors propose an innovative on-body RecCoil array harvester with a central receiver (Rx) coil to capture longitudinal field components and four auxiliary side Rx coils to encapsulate lateral field components, each formed by two oppositely wound circular coils and integrated with full-bridge rectifiers. The rectified outputs are combined using a DC technique. The Rx coil is EM-optimized to harness three orthogonal H-field components from the Tx coil, ensuring uniform voltage and Power Transfer Efficiency (PTE) across the Rx plane at a 50 mm altitude. Simulation results indicate that the lateral misalignment tolerance of the proposed structure decreases with increasing altitude beyond 50 mm. The design improves measured PTE to 72.22% (aligned) and 70.91% (misaligned), outperforming the conventional Rx coil's PTE of 50.13% and 17.01%, respectively. Furthermore, it is seamlessly integrated with the PCB-based charging circuitry

	to validate and demonstrate the battery charging process effectively. Because it weighs 20 g lower than its competitors, its flying efficiency won't be compromised, thereby providing a superb misalignment charging (offset between the Tx and Rx) of 100% at 50 mm for the quadcopter with good PTE, given the well-organized and optimized RecCoils to well-matched full AC-DC rectification. The dynamic tests for drone charging will be considered as a part of future works.
31.	Analyzing PCM melting front propagation for energy optimization in hot climate roofing: experimental approach **JA Peerzada, M Subramaniyan** - Journal of Thermal Science, 2025 **Abstract:** The rapid commercialization of Phase Change Materials (PCMs) for HVAC applications effectively leverages ambient temperature fluctuations to meet growing energy demands in buildings. This study outlines a systematic approach to passively integrate PCM into building roofs for cooling load reduction. The process involves PCM selection, characterization, analysis of melting front propagation, and thermal performance assessment. Thermal/digital imaging approach tracks the melting front's propagation, revealing significant natural convection due to heat flux from modules bottom surface. Melting front propagation occurs primarily in one dimension. Two identical roof slab units are fabricated and tested in Rupnagar City, India, for assessing thermal performance, with one unit equipped with PCM (PSU) and the other as a conventional reinforced slab unit (CSU). Various energetic and thermal performance metrics, including Maximum Temperature Reduction (MTR), Operative Temperature Difference (OTD), Heat transfer, electricity cost savings (Esc), Discomfort Hours Reduction (DHR), and Maximum Heat Gain Reduction (MHGR), are evaluated. PCM integration results in a significant MTR of 4°C and a 60% reduction in heat flux compared to the conventional unit. Moreover, the PCM room exhibits an 11.2% and 34.8% enhancement in thermal comfort, as indicated by DHR and MHGR, respectively, compared to the reference unit. In addition, considering heating and cooling spaces, it offers a maximum daily saving of 0.06 USD/(kWh·m^2). These findings highlight PCM's potential to mitigate temperature fluctuations, enhance thermal comfort, and reduce energy consumption in severe climatic conditions.
32.	Application of the variance gamma distribution for change point detection **M Rani, B Garg, A Kumar** - Communications in Statistics-Simulation and Computation, 2025 **Abstract:** This article explores the application of the variance gamma distribution for detecting change points in financial data. Unlike conventional two-parameter and three-parameter distributions, the four-parameter variance gamma distribution uniquely captures skewed and heavy-tailed dynamics of daily financial returns. We conduct Monte Carlo simulations under the null hypothesis of no change in distribution parameters to find critical values of the likelihood ratio test and the modified information criterion procedures for change point detection. Simulation studies are also conducted to compare the effectiveness of these procedures. A power analysis is utilized to assess their comparative performance. Since power comparison results indicate the superiority of the modified information criterion over the likelihood ratio test, we work with the modified information criterion to detect change points in real-world datasets. We consider daily log returns of four stock indices: Nikkei 225, Hang Seng Index, OMX Stockholm 30, and NIFTY 50. Multiple change points are detected in these datasets using binary segmentation. These points are further analyzed to provide insights into shifts in financial market dynamics. Our findings highlight that the detected change points align with various macroeconomic shocks related to the 2020 pandemic, interest rates, crude oil prices, inflation rates, political uncertainty, and many others.

33.	Automated mapping of glacial lakes in Himachal Pradesh using multi source remote sensing data and machine learning B Pathak, A Singh, **RK Tiwari**, DP Shukla - Scientific Reports, 2025 **Abstract:** The Himalayas are undergoing active climate-induced changes, resulting in glacial lake formation and expansion. Glacial lakes are important reservoirs of freshwater but also run the risk of glacial lake outburst floods (GLOFs). As sentinels of climate change, dynamic monitoring of glacial lakes is necessary. This research introduces an automated method for mapping glacial lakes in Himachal Pradesh based on multi-source remote sensing data and a random forest (RF) classifier. The model was tested under various scenarios using spectral bands and remote sensing indices extracted from Sentinel-2 and Planet images. The combination of Sentinel-1 SAR, Sentinel-2 MSI, and SRTM DEM data resulted in a classification accuracy of 93.69%, which increased to 94.44% with the addition of high-resolution Planet images. Although the method was effective in identifying glacial lakes, it faced difficulties in distinguishing glaciers from supraglacial lakes. Postprocessing methods were used to enhance the results. Model performance was evaluated using statistical measures, such as recall, precision, F1-score, and overall accuracy. The RF classifier performed well robustly, identifying its reliability in glacial lake mapping even being a machine learning method.
34.	Aza-triphenylene-based covalent organic framework: Anode for high-efficiency sodium-ion batteries **M Kaur**, B Chakraborty, **TJD Kumar** - Journal of Energy Storage, 2025 **Abstract:** This research examines the suitability of newly synthesized aza-triphenylene based covalent organic framework (aza-COF) as a negative electrode material for sodium-ion batteries (SIBs) through first-principles density functional theory. This work identifies the two-dimensional aza-COF as a direct band gap semiconductor with an energy gap of 1.02 eV. When sodium is loaded at the most reliable location, the aza-COF system changes from a semiconductor to a metallic state, leading to improved electrical conductivity. Aza-COF shows a diffusion barrier of 0.78 eV, a high theoretical specific capacity of 602.3 $mAhg^{-1}$, an energy density of 1259.5 $mWhg^{-1}$, and mean voltage of 0.62 V falling within the ideal range of 0.1–1.0 V. Additionally, its structural adaptability further supports its suitability for such applications. Also, aza-COF demonstrates a strong affinity for electrolytes highlighting its exceptional suitability for electrode applications. These compelling theoretical results indicate that aza-COF could function as a highly efficient anode material for SIBs. 

35.	Breast cancer awareness and its predictors among university students and employees in Asir region, Saudi Arabia: a cross-sectional study U Hani, M Manzoor… **JA Malik**…AA Fatease - Scientific Reports, 2025 **Abstract:** Breast cancer (BC) is the most common cancer and the leading cause of cancer-related deaths in Saudi Arabia. However, this malignancy can be tackled effectively with early detection, resulting in better patient outcomes and reduced mortality rates. Breast screening, whether self-screening or clinical screening, plays a pivotal role in early BC detection. Hence, understanding, knowledge, and perception of BC and its risk factors are very important in early BC diagnosis. The current study has been conducted to assess the understanding, knowledge, perception, and attitude of educated population of Asir region towards BC and its risk factors. The study was conducted among the participants aged 18 or above in various institutions of the Asir region in KSA using an online pre-validated questionnaire to assess the understanding, knowledge, and perception of BC and its risk factors. The study was completed by a total of 979 participants. The proportion of participants who demonstrated adequate knowledge and positive perception regarding the role of breast self-examination and early detection was greater than 50%, indicating an overall satisfactory level of breast cancer awareness among the study population. However, in identifying the risk factors of BC, < 50% of participants correctly identified the 8 correct risk factors out of 12. When analyzing the association of BC awareness with demographic characteristics, the results revealed that females had 2.012 times higher odds of BC awareness than males. Additionally, participants with higher education qualifications had 3.867 times higher odds of BC awareness than those with bachelor's degrees. Also, the results show that demographic factors like female sex, age, marital status, urban residence, occupation (administrative staff), and higher education level were associated with the level of knowledge about breast cancer risk factors. Participants demonstrated generally good knowledge and perception of breast cancer, particularly regarding early detection and available screening tools. However, awareness of breast cancer risk factors was notably limited. Therefore, there is a clear need for targeted and region-specific awareness programs to enhance understanding and promote early intervention.
36.	CFD-DEM modeling of fluidized bed granulator: Granule formation, identification, and evolution of granule size distribution A Rajput, J Chakraborty, **J Kumar**, A Tripathi - Powder Technology, 2025 **Abstract:** The present study adopts a CFD-DEM coupled approach for modeling the wet granulation in a sparse pseudo-2D fluidized bed of dry and wet spherical particles. The granules formed through particle interactions are quantified using a novel granule identification algorithm, by accounting for the particle curing period and the surface liquid content. The identified granules are replaced by a multi-sphere model to incorporate the effect of granule strengthening due to drying of the liquid bridge. The temporal evolution of granule size distribution is analyzed, and the effects of key process parameters, including superficial gas velocity, liquid binder properties (such as liquid content, viscosity, and surface tension), and curing period, are investigated. Among various factors explored, the liquid binder surface tension and superficial gas velocity are found to be the strongest factors. Viscosity does not seem to play a significant role, possibly due to the use of coarse-grained particles. 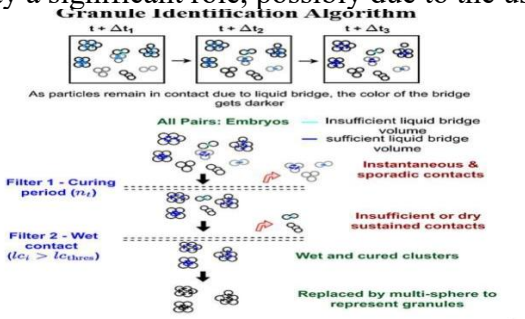

37.	Compact convolution transformer with cross-feature aggregation for hand-gesture recognition S Narayan, P Hambarde, **SK Vipparthi**, AP Mazumdar, S Murala - Computers and Electrical Engineering, 2025 **Abstract:** Hand Gesture Recognition (HGR) plays a crucial role in intuitive human–computer interaction but continues to face challenges such as complex backgrounds, lighting variations, occlusions, and limited training data. To overcome these issues, we propose a Cross Feature Aggregation Compact Convolution Transformer (CrFe-CCT) that integrates multiscale convolutional features with a lightweight transformer architecture. In the proposed CrFe-CCT network, includes the multi-scale Cross Feature Aggregation (CrFe) and CCT modules. The CrFe module help to enhances feature robustness by fusing contextual information across scales, leading to improved recognition accuracy while maintaining low computational complexity. Also, CCT module help to preserve local spatial relationships. Unlike conventional transformers that rely on large-scale data, CrFe-CCT enables efficient learning on both small and large datasets. The experimental results demonstrate that the proposed CrFe-CCT outperforms existing state-of-the-art approaches on subject-dependent datasets, achieving accuracies of 91.95%(HGR-1), 97.70% (MUGD Set1), 95.50% (MUGD Set2), 99.06%(MUGD Set3), 99.82% (NUS-II), 99.90% (ASL-Finger Spelling (FS), and 96.80% (OUHands). On subject-independent datasets, the CrFe-CCT network achieves 40.43%(HGR-1), 85.11% (MUGD), 70.34 (NUS-II Dataset), 82.20% (ASL-Finger Spelling (FS)), respectively. Furthermore, it demonstrates superior efficiency with parameters, memory usage, FLOPs, inference time, and a throughput of images for real-world HGR applications.
38.	Computational heat transfer analysis of oxide nanofluids around a fixed heated cylinder S Javed, **HVR Mittal**, P Kumar, S Saranya… - International Journal of Thermofluids, 2025 **Abstract**: Nanofluids are helpful to improve the effectiveness of thermal systems for different industries, which helps in producing energy in an environmentally sustainable manner, downsizing the systems and enhancing profitability. In this study, the heat transfer characteristics of a nanofluid flowing over a circular cylinder with an axisymmetric heated surface were investigated. Three nanofluids based on the above materials suspended in the water with the volume fractions of the particles equal to 0% to 0.05% respectively, have been used in order to do comparison. The time dependent equations here targeted for simulation are the Navier-Stokes equations of motion in three dimensions. The numerical simulations were performed for a Reynolds number Re = 200, 0∘ ≤ θ ⁀ ≤ 180∘ and Pr = 6.2. The two-dimensional momentum and energy conservation equations were solved (numerical analysis), while varying the order of compact HOC on non-uniform polar grids. Different types of the nanoparticles were used to disperse in the heat conducting fluid in order to understand how the thermal fields in the cylinder would be developed. The results reveal that the application of nanoparticles improves heat transfer by a greater measure because it increases the Nusselt number which reflects greater convection and conduction. The highest Nusselt numbers are recorded at the stagnation point, where convective heat transfer reaches its maximum in accordance with the level of shear. The thermal conductivity of Al2O3 and SiO2 nanoparticles raise the heat transfer rate, and so does the proper selection of concentration of applied nanoparticles, which is required to enhance the thermal efficiency of the cooling system.
39.	Counter-memory as resistance: Reading second-generation holocaust fiction in thane Rosenbaum's second hand smoke (1999) and the golems of Gotham (2002) **SC Balakrishnan, A Nandha** - Journal of Modern Jewish Studies, 2025 **Abstract:** Using George Lipsitz's and Verónica Tello's discourses on counter-memory, this paper examines the representation of second-generation Holocaust survivors by analyzing Thane Rosenbaum's *Second Hand Smoke* and *The Golems of Gotham*. The article analyzes characters who resist normative historical narratives by crafting their own disparate counter-memories as a tool to broaden and reframe history. Here, the second-generation characters engage with memory in ways that challenge the collective aggregates of canonical history and memory. This paper positions the second-generation's traumatic experiences against dominant accounts and reveals a parallel narrative of resistance that emerges consequently. The novels illustrate that the second-generation can initiate reconciliation by resisting rigid official histories and rejecting the imposed identity as passive

	custodians of transferred memories. Ultimately, the second-generation finds reprieve in building an identity that transcends solely being children of survivors. In reframing the collective memory of the Holocaust to include its aftermath on the later generations, these counter-memories encourage positioning it as an unresolved tragedy – one that continually requires critical engagement and reconciliation.
40.	Design and analysis of low-complexity communication receiver for PSK-LFM joint sensing and communication waveform **D Salwan, S Agarwal, B Kumbhani** - IEEE Transactions on Intelligent Vehicles, 2025 **Abstract:** In this article, we propose novel strategies for preamble detection and synchronization to detect the symbols from the phase shift keying-linear frequency modulated (PSK-LFM) joint sensing and communication waveform at the communication receiver of an unmanned aerial vehicle (UAV). Since radar waveform requires huge bandwidth (order of 100 MHz–2 GHz) for better range resolution, processing the same waveform at the UAV's communication receiver necessitates high analog-to-digital converter (ADC) sampling rates. To reduce the ADC sampling requirements, in this paper, we propose two signal processing schemes for the communication receiver. In first, a part of the received signal is filtered using a low pass filter (LPF) and sampled for preamble detection, symbol synchronisation, and detecting the symbols. In the other case, the entire signal undergoes under sampling for subsequent processing. Furthermore, we obtain bit error rate (BER) performance for all the cases by considering time, phase, and carrier frequency offsets. We show that processing the undersampled signal yields superior BER performance compared to the filtering approach, even when both operate at an equivalent sampling rate. Furthermore, for all cases, we compare the simulation results with and without offsets, along with the analytical results obtained without offsets.
41.	Design of planar 2D Semiconductors incorporating sp^2-hybridized group 13 metals with boron, carbon, and nitrogen Z Zhang, K Leifer, **R Ahuja**, W Luo - Nano Energy, 2025 **Abstract:** The sp^2-hybridization is key to understand structures of 2D materials with light p-block elements. However, hunting for sp^2-hybridized 2D materials with heavy p-block elements remains challenging due to weaker π-bonding and increased steric effects. Here we proposed design principles for 2D materials based on carbon nitride with adjacent Lewis-acidic center of group IIIA elements. We introduce a family of 2D materials $XB_9C_4N_6$ (X = Al, Ga, In and Tl) with high thermodynamic stability. Density functional theory (DFT) calculations reveal that $XB_9C_4N_6$ exhibit a polycyclic lattice with high delocalized π electrons, primarily from B_6 ring, which play the key role in the hole and electron transports. These materials exhibit small electron effective mass of ~ 0.28 m_0, suitable bandgaps of ~ 1.2 eV and strong light absorption peaks of violet, red and near-infrared lights, which cover the solar spectral irradiance. Notably, $AlB_9C_4N_6$ emerges as an environmentally friendly semiconductor for electronics and photovoltaic devices. The design principles will enrich the fundamental understanding of π-conjugated heavy p-block elements and family of sp^2-hybridized 2D materials. 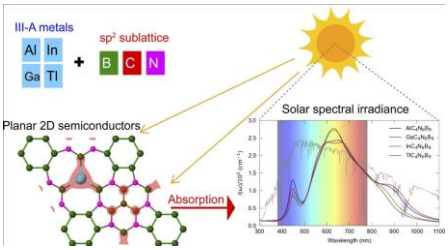
42.	Disordered open plasmonic cavities for broadband emission enhancement of nitrogen-vacancy center **N Singh, H Sammi, N Ahmed, N Sardana, RV Nair** - Advanced Optical Materials, 2025 **Abstract:** The unique optical and spin properties of nitrogen-vacancy (NV) centers have revolutionized the possibilities of room-temperature quantum technologies. However, the applicability of NVs can be further enhanced by coupling them with plasmonic structures. Here, the integration of a few NVs is discussed with disordered open plasmonic cavities made of gold for broadband emission enhancement at room temperature. The study involves a statistical analysis of

	coupled NVs, revealing accelerated emission rates and enhanced intensity with scalability, long-term stability, and reproducible emission properties. The disordered open cavities enhance the spontaneous emission decay rate by a factor of five by enhancing the local density of optical states, supported by numerical simulations. The extent of enhancement depends on the spatial variation in nanopore size, affecting mode volume in the proximity of NVs. The statistical variation in the estimated pore size is directly related to the measured lifetime distribution, implying the robustness of the disordered sample over a large area with strong emitter-cavity coupling. The results are useful to enhance the sensitivity of NV-based quantum sensors and to realize bright single-photon sources. The structure is also suitable for many other quantum emitters with slow emission rates and for developing room-temperature quantum technologies.
43.	Dynamic control of electromagnetically induced transparency in a toroidal planar terahertz metasurface LK Vaswani, KM Rohith…**S Ghosal**…**G Kumar** - IEEE Journal of Selected Topics in Quantum Electronics, 2025 **Abstract:** The dynamic control of terahertz (THz) transmission is crucial for next-generation devices, including sensors, modulators, and slow-light systems. This study investigates an actively tunable electromagnetically induced transparency (EIT) effect in a toroidal dipole-based THz metamaterial. Experimental and numerical analyses confirm toroidal excitation through surface current distributions, profiles of the magnetic field, and multipolar analysis. The metamaterials, fabricated on a flexible polyimide substrate, achieve tunable modulation of EIT using vanadium dioxide (VO2). The terahertz time-domain spectroscopy in transmission mode reveals modulation efficiency of up to 50%. Additionally, active control of group delay is demonstrated, highlighting the versatility of the proposed design for advanced THz applications.
44.	Dynamics of an internally actuated weakly elastic sphere translating parallel to a rigid wall **S Verma**, B Dinesh, **NK Marath** - Journal of Fluid Mechanics, 2025 **Abstract:** We analyse the dynamics of a weakly elastic spherical particle translating parallel to a rigid wall in a quiescent Newtonian fluid in the Stokes limit. The particle motion is constrained parallel to the wall by applying a point force and a point torque at the centre of its undeformed shape. The particle is modelled using the Navier elasticity equations. The series solutions to the Navier and the Stokes equations are used to obtain the displacement and velocity fields in the solid and fluid, respectively. The point force and the point torque are calculated as series in small parameters α and 1/H, using the domain perturbation method and the method of reflections. Here, α is the measure of elastic strain induced in the particle resulting from the fluid's viscous stress and H is the non-dimensional gap width, defined as the ratio of the distance of the particle centre from the wall to its radius. The results are presented up to O(1/H3) and O(1/H2), assuming α∼1/H, for cases where gravity is aligned and non-aligned with the particle velocity, respectively. The deformed shape of the particle is determined by the force distribution acting on it. The hydrodynamic lift due to elastic effects (acting away from the wall) appears at O(α/H2) in the former case. In an unbounded domain, the elastic effects in the latter case generate a hydrodynamic torque at $O(\alpha)$ and a drag at $O(\alpha 2)$. Conversely, in the former case, the torque is zero, while the drag still appears at $O(\alpha 2)$. 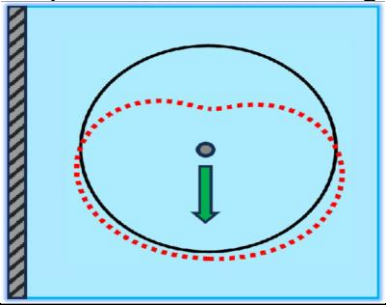
45.	Electron donor-acceptor complex offers a diverse approach for carbonyl alkylative amination **H Paul, A Chakraborty, A Mandal, D Das**…**I Chatterjee** - Chemical Science, 2025 **Abstract**: The synthesis of α-tertiary amino acids and amines is crucial in biochemistry and medicinal chemistry. However, creating tertiary carbon centers has traditionally been challenging due to the

	lack of effective, sustainable, and straightforward mild protocols. This current work presents a method for creating α-tertiary carbon centers that leverages the formation of an electron donor-acceptor (EDA) complex, where electron-poor imines act as the acceptor and electron-rich 1,4-dihydropyridine serves as the donor. This interaction facilitates the generation of α-amino radicals through a charge transfer phenomenon. In the presence of a suitable radical trapping reagent, these α-amino radicals can forge C-C bonds, where H-DHP acts solely as a reductant. Additionally, a radical cross-coupling process between an alkyl radical generated from 4-alkylated 1,4-dihydropyridine and the α-amino radical also produces reductive alkylation products. In this later scenario, 4-alkylated 1,4-dihydropyridine functions both as a reductant and as a source of alkyl radicals. Interestingly, both processes yield amino acids and amine derivatives having α-tertiary centres under mild reaction conditions, avoiding the need for photocatalysts or transition metals.
46.	Engineering epsilon-near-zero response and polarization-independent radiative ferrell-berreman modes in nanoporous gold-silver films **J Singh**, NK Gupta, **S Sarkar** - Journal of Physics D: Applied Physics, 2025 **Abstract:** Ferrell and Berreman modes, arising from radiative bulk plasmon-polariton and phonon-polariton excitations, are absorption resonances in thin metal films and polar-dielectric media. These modes characterized by volume charge oscillations and epsilon-near-zero (ENZ) characteristics offer unique light–matter interaction pathways and have thus garnered extensive research interest. Here, we demonstrate nanoporous gold–silver (NPGS) films as a versatile platform for realizing Ferrell–Berreman (FB) random metasurfaces with thickness-dependent ENZ response control. Experimentally, we extract the effective optical constants of NPGS films with varying thicknesses, enabling precise tuning of ENZ points from visible (600~ nm) to near-IR (900~ nm) wavelengths. Further, we show, due to the bicontinuous and random anisotropic nature of the films, the excitation of FB modes near the ENZ wavelength exhibits polarization-indiscriminate behavior. To theoretically validate these findings, we employ a hybrid effective medium approximation that combines the Maxwell–Garnett (MG) and Bruggeman (BR) models. The MG model addresses optical scattering from surface roughness, while the BR model captures the effects of porosity on the material's optical properties. This hybrid model in light of the statistically anisotropic nature of NPGS films enables us to quantify the effective permittivity and corroborates well with the experimentally observed polarization indiscriminate resonances observed near the ENZ wavelength.
47.	Evaluation of semiprocess-based and empirical models in simulating root water uptake under water- and salt-stressed conditions **A Kumar, I Sonkar** - Journal of Irrigation and Drainage Engineering, 2026 **Abstract:** The transpiration reduction function of root water uptake (RWU) models play a crucial role in modeling crop evapotranspiration, yield, and water-use efficiency. Various empirical functions can describe how RWU responds to water and salt stresses. This study evaluated semiprocess-based (McS) and empirical RWU models that are sufficiently sophisticated to model salt-water dynamics under stress conditions. Global sensitivity analysis was performed on these models for an irrigated scenario of berseem (*Trifolium alexandrinum*) for a numerical crop growth experiment. The sensitivity of the model outcomes (relative transpiration, bottom flux, and average root zone electrical conductivity) to soil hydraulic and stress parameters was analyzed. The results show that the model outcomes were more sensitive to the threshold stress parameters of the McS model than to those from the empirical models. The McS model's cumulative bottom flux (CBF), average root zone electrical conductivity, and relative transpiration (RT) information emerged as effective data for parameter calibration, whereas other models fell short in addressing uncertainties related to water stress parameters. The observed increase in uncertainty during deficit irrigation in saline soil emphasized the importance of accurately characterizing stress parameters to enhance the predictive capabilities of the model developed. The model effectively simulates water deficit and salinity impacts on RWU, showing strong sensitivity to stress parameters, particularly in dry periods and deeper root zone layers. The McS model parameters were calibrated using berseem data, and showed good alignment with observed soil moisture ($R2$=0.74–0.86) and electrical conductivity ($R2$=0.86–0.92) at various depths. The model effectively characterizes stress parameters, thereby enhancing predictive capabilities for RWU dynamics under water deficit and saline conditions.

48.	Explicit representation of surface water bodies in regional groundwater flow: an analytical solution for layered heterogeneous aquifers **M Das, S Maurya, R Sarmah** - Modeling Earth Systems and Environment, 2026 **Abstract:** Accurately predicting regional groundwater flow behavior in layered, heterogeneous aquifers remains a central challenge in hydrogeology. This study presents an analytical model for steady-state groundwater flow in a stratified three-layer aquifer system with anisotropic, depth-dependent hydraulic conductivity. Unlike prior models, this approach incorporates both a water table and surface water bodies as top boundary conditions over a finite vertical domain, addressing key limitations of earlier semi-infinite or topography-constrained frameworks. The model employs an exponentially decaying conductivity profile within each layer and utilizes a separation-of-variables solution technique to derive an analytical expression for hydraulic head. Validations against the existing analytical solution and COMSOL-based numerical simulation demonstrate strong agreement. The framework further enables analysis of recharge/discharge zones, artesian conditions, stagnation points, and groundwater particle travel paths across varied hydrogeological scenarios. The model reveals several novel insights, including the emergence of dual recharge–discharge behavior beneath surface water bodies due to climate variability, fragmentation of the groundwater flow system, and the presence of stagnation zones influenced by boundary conditions and conductivity structures. Key findings highlight the significant influence of surface water body boundaries and vertical heterogeneity on flow paths and artesian conditions. Sensitivity analysis identifies vertical conductivity of upper-layer as key drivers of hydraulic head variation. Additionally, residence time distributions exhibit heavy tails, with the Fréchet distribution providing the best statistical fit. It fills a key knowledge gap by showing how aquifer stratigraphy governs subsurface water connectivity and enables long-distance contamination via preferential flow paths, intensified by climate-induced waterbody shrinkage.
49.	Exploring the patterns of bacterial interactions with the other **R Joy** - Biosemiotics, 2025 **Abstract:** This review article explores the concept of the bacterial *other* by highlighting numerous ways bacteria recognize and interact with organismal and non-organismal entities in their environment. It expounds two patterns of bacterial otherness by drawing multiple examples from basal cognition and sociomicrobiology. These two patterns are the non-organismal other, i.e., the physical entities in the bacterial environment, and the organismal other, the living entities in the bacterial environment. By detailing numerous processes such as chemotaxis, learning, memory, kin recognition, altruism, predation, and cooperation, and analyzing these patterns of bacterial interactions, this review article also attempts to make a case for microbial bodily self.
50.	Firm investment, financial constraints and agency costs: evidence from India **MA Vincent**, PK Das, **S Bardhan** - Empirical Economics, 2025 **Abstract:** The investment slowdown among Indian firms is a pressing concern with far-reaching implications for the nation's growth trajectory. Against this backdrop, the present study investigates how finance constraints and agency costs impact firm-level investment efficiency. Based on the Prowess database of Indian private manufacturing firms between 1999 and 2024, we employ two-tier stochastic frontier model (2TSFM) with intra-error dependence to analyse investment inefficiencies arising from under-investment (due to finance constraints) and over-investment (due to agency costs). Our results reveal a significantly negative association between finance constraints and investment, and a significantly positive association between agency costs and investment. Firms with lower agency costs face lesser finance constraints, enabling them to invest more; however, as agency costs increase, this positive effect diminishes, indicating that even some firms with high agency costs still manage to secure external funding. These findings highlight the need for targeted reforms in firm financing and corporate governance to enhance investment efficiency and foster sustained economic growth in emerging economies such as India.

51.	Forecasting inclusive futures: Fintech, capability expansion, and livelihood pathways in urban Indian slims- a mixed-methods analysis **J Singh**, GS Batra, S Kaur - Technological Forecasting and Social Change, 2025 **Abstract:** Rigorous evidence forecasting fintech's poverty alleviation mechanisms in low-income settings remains scarce. Integrating Sen's Capability Approach and the Sustainable Livelihoods Framework, this study analyzes fintech's influence on productive credit use, assets, and capabilities in Indian slums. A mixed-methods design ($N = 600$ survey, 40 interviews) combines Structural Equation Modeling (SEM) and fuzzy-set Qualitative Comparative Analysis (fsQCA). SEM confirms fintech adoption strongly predicts productive credit use ($\beta = 0.68$, $p < 0.001$), fostering assets ($\beta = 0.72$) and capabilities ($\beta = 0.75$), improving livelihoods ($\beta = 0.70$); policy support significantly moderates ($\beta = 0.30$, $p = 0.002$) the initial fintech-credit link. Complementing SEM's net effects, fsQCA reveals two sufficient, equifinal pathways to improved livelihoods: (1) high fintech adoption *with* robust policy support (Consistency: 0.87, Coverage: 0.42), demonstrating policy synergy, and (2) moderate fintech usage *compensated by* strong social networks and prior assets (Consistency: 0.82, Coverage: 0.31), highlighting community compensation mechanisms. Qualitative data illuminate crucial roles of trust, digital literacy, mentorship, and gender dynamics, a finding quantitatively substantiated by a multi-group analysis revealing that women are significantly more effective at leveraging social networks, while revealing risks such as digital exclusion and potential debt traps. Findings forecast that successful fintech deployment for poverty reduction necessitates synergistic socio-technical ecosystems—combining technology with enabling policies, community structures, and proactive mitigation of negative externalities—thereby informing strategies for inclusive, sustainable social change. 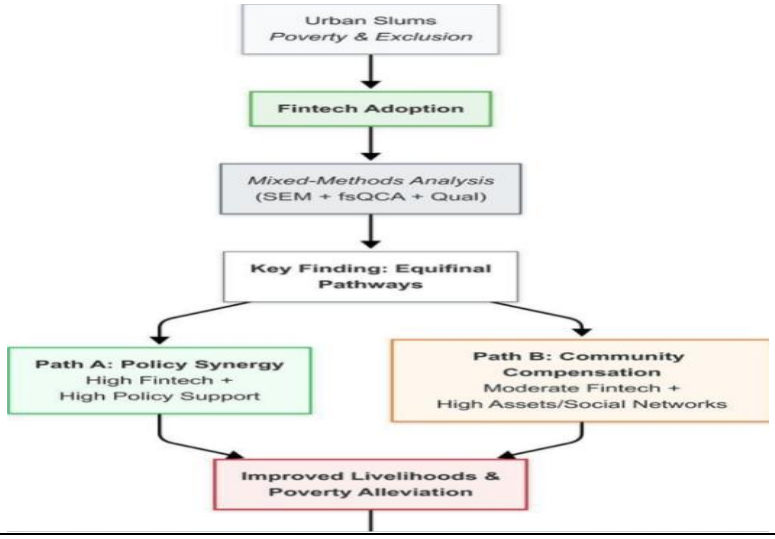
52.	Fretting wear mechanism of plasma-sprayed CNT-reinforced wollastonite-zirconia composite coatings for bioimplant applications A Kumar, **S Rathor**, S Singh, **R Kant**, **H Singh**… - Tribology International, 2025

	Abstract: This study investigates the fretting wear mechanisms of plasma-sprayed wollastonite-zirconia ($CaSiO_3$-ZrO_2, WaZr) composite coatings, both unreinforced and reinforced with carbon nanotubes (WaZr-CNT), for bioimplant applications. The developed coatings are compared with conventional hydroxyapatite (HA) coatings on titanium substrates. Microstructural analysis reveals that CNT reinforcement leads to a denser, more uniformly bonded WaZr-CNT coating through effective splat bridging and pore sealing. Mechanical characterization shows that WaZr-CNT coatings possess higher microhardness and lower elastic modulus than unreinforced WaZr coating. During fretting tests at a 200 µm displacement amplitude, the WaZr-CNT coating exhibited an approximately 83 % reduction in energy dissipation compared to HA coatings and a 75 % reduction compared to WaZr coatings, indicating significant improvement in fretting resistance. While HA and WaZr coatings underwent splat fracture and generated considerable amount of wear debris, the WaZr-CNT coating produced almost no debris and maintained intact splat boundaries. The novelty of this work lies in the development and evaluation of CNT-reinforced WaZr coatings that for the first time undergo fretting tests and demonstrate superior fretting wear resistance under cyclic sliding contact compared to unreinforced WaZr and conventional HA coatings.
53.	From molecules to mechanisms: Integrating MD and stochastic modeling to decipher RXR-RAR gene regulation **N Kumar, D Kashyap**, P Khatua, **SK Sinha** - The Journal of Physical Chemistry B, 2025 **Abstract:** This study integrates atomistic molecular dynamics (MD) simulations with stochastic modeling to unravel the gene regulatory mechanism mediated by nuclear receptors (NRs), ligand-activated transcription factors. We specifically study the heterodimeric RXR-RAR nuclear receptor system. We use MD simulations to investigate ligand-induced allosteric communication, receptor dynamics, and DNA recognition. The results suggest that receptor dimerization precedes DNA binding, and even single-ligand occupancy induces allosteric signaling that stabilizes the complex, indicating ligand binding as a modulator of gene expression. In contrast, we propose a ligand-induced downregulation mechanism of gene expression that involves disruption of allosteric pathways, weakening of the receptor–DNA interface, and promotion of complex dissociation, as inferred from binding free energy calculations. To bridge the time scale gap between molecular events and gene-level regulation, we integrate MD-derived data into a stochastic modeling framework to construct an NR-mediated gene regulatory network. This analysis reveals that ligand-specific allosteric activation predominantly drives gene expression. The results further demonstrate that the system maintains an ordered transcriptional response despite noisy intermediate dynamics, ensuring minimal mRNA production through a balance between synthesis and degradation. This integrated approach connects molecular-scale interactions with long-time scale regulatory dynamics, providing mechanistic insights into NR-mediated regulation. Using RXR-RAR as a representative system, we establish a computational framework to explore the principles of NR function and dysfunction that are often inaccessible through experiments or conventional MD simulations. 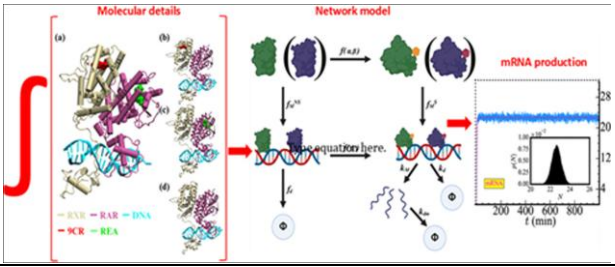

54.	GOPAL: A water model with improved thermodynamic properties over a large pressure and temperature range optimized using multistate reweighting and configuration space mapping **H Paliwal**, MR Shirts - Journal of Chemical Theory and computation, 2025 **Abstract:** We show how reweighting and configuration mapping algorithms can be used to efficiently optimize molecular models using thermodynamic properties at a large number of state points from molecular simulations. As a proof of concept, we perform a multidimensional, multiobjective parameterization of a rigid water model over a large pressure [1–5000 atm] and temperature [274.15–372.15 K] range to the experimental property surfaces estimated using the IAPWS95 equation of state for water. Over 4000 parameter combinations in a six-dimensional parameter space were explored during the minimization. A similar parameterization with standard techniques would have taken more than 250 CPU years, but with the application of the newly developed techniques, the computational time was reduced to four CPU months. Without the added efficiency of the methods presented here, the optimization could not have simultaneously taken into account the large range of temperature and pressure points used in the fitting. The paper also describes how and why incorporating the thermodynamic properties from the first and second derivatives of Gibbs energy into the objective function helps improve the parameterization process. The resulting water model reproduces liquid phase density within the upper limit of experimental uncertainty of 0.02% over a large range of temperatures and pressures, the most accurate model yet at this low level of theory over the entire range of temperature and pressure, with little loss of fidelity in other properties. We compare the performance of this water model with 11 other rigid water models in predicting a number of other thermodynamic and kinetic properties. This process illustrates the surprising fact that a simple point charge model is able to accurately capture a substantial range of both temperature- and pressure-dependent thermodynamics without substantial deviation from experiment at ambient temperatures and pressures.
55.	Harnessing imperfection: Deep learning-based receiver for non-coherent distributed transmission **A Ahmad, S Agarwal, S Kaur, SS Jha**, GC Prabhunath - IEEE Transactions on Cognitive Communications, 2025 **Abstract:** This paper investigates the feasibility of distributed multi-transmission in non-coherent systems using deep learning (DL), a concept we term non-coherent distributed transmission (NCDT). In this approach, multiple transmitters non-coherently send the same content to a receiver. We leverage DL to learn and capture the complex patterns arising from signal combinations with frequency and phase offsets. By engineering relevant features and designing a deep neural network with an adaptable auto-tuning mechanism, we enable precise mapping of received signals to transmitted symbols within the NCDT framework. Additionally, we develop a likelihood ratio test (LRT)-based detector as a baseline for comparison. Our simulations and experiments demonstrate that the proposed DL-based receiver achieves lower bit error rates (BER) than the other state-of-the-art DL-based and LRT-based detectors while eliminating the need for synchronization, channel state information (CSI) estimation, or precoding. Experimental validation using software-defined radios corroborates our simulation results, confirming that NCDT can be practically integrated into wireless systems without requiring hardware modifications. Notably, our results show that the proposed method achieves comparable BER performance at nearly half the transmission power, corresponding to an approximate 3 dB gain.
56.	In situ formed polyvinylsilazane-derived SiCN-reinforced aluminum matrix composites with enhanced properties **V Girish C**, **R Bura**, **H Singh, RM Prasad** - Journal of the American Ceramic Society, 2025

	Abstract: In this work, a polyvinylsilazane was in situ pyrolyzed to disperse amorphous SiCN phase as reinforcement in aluminum matrix composites by ex situ cross-linking of polymer at 300°C followed by mixing with molten aluminum in a bottom pouring stir casting setup. Composites having 2–6 wt% in situ formed SiCN were synthesized by adding required amounts of cross-linked polymer which underwent in situ pyrolysis transformation at 800°C under inert atmosphere. Structural characterization of the synthesized composites were conducted using X-ray diffraction (XRD), Fourier transform infrared spectroscopy (FTIR), and field emission scanning electron microscopy (FESEM). Significant enhancement in mechanical properties were found for the composites compared to pure aluminum, such as hardness (by ~78%), ultimate tensile strength (by ~120%), and compressive strength (by ~172%) for aluminum matrix composite reinforced with 4 wt% SiCN.
57.	Influence of multi-walled carbon nanotubes on the structure and conductivity of electrospun PAN-based carbon nanofibers R Sharma, N Arya, K Kumari, **G Uppal, R Kumar**… - Materials Today Chemistry, 2025 **Abstract:** This work reports the fabrication of polyacrylonitrile (PAN)-derived carbon nanofibers (CNFs) reinforced with 0.25 wt% multi-walled carbon nanotubes (MWCNTs). Carbonization at 1000 °C significantly enhances graphitization, mitigates structural defects, and optimizes the electronic structure, yielding conductivity improvements usually achieved only at 1100–1700 °C. Fermi-level analysis showed enhanced sp^2 bonding and π-electron delocalization, while defect suppression stabilized the σ-bond framework, reinforcing conductivity. The optimized CNF@CNT composite exhibited lower resistivity (11.53 vs. 25.16 mΩ cm for pristine CNFs) and superior electronic performance. Raman confirmed improved graphitic ordering (La: 3.66 vs. 4.0 nm), XRD indicated modified crystallite parameters (Lc: 0.96 vs. 1.20 nm; d002: 0.371 nm), and XPS revealed a higher sp^2/sp^3 ratio (76.16 vs. 72.09). TEM showed an amorphous 002 feature, and SEM revealed reduced fiber diameter (130 vs. 140 nm). Electrical tests demonstrated a tenfold current increase (~100 vs. ~10 μA), with successful LED integration validating practical conductivity. This strategy lowers processing temperature, minimizes CNT use, and enables scalable, cost-effective fabrication of high-performance CNFs for flexible and room-temperature electronics. 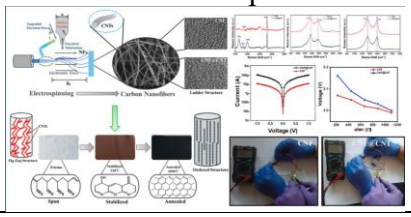
58.	Interfacial engineering of nanoparticles and nanoflakes via bridged microreactors M Tiwari, **M Sabapathy**, MG Basavaraj, VR Dugyala - Colloids and Surfaces A: Physicochemical and Engineering Aspects, 2025 **Abstract:** Bridged emulsion, wherein the droplet surface is partially covered with solid particles, is demonstrated as an efficient pathway for interfacial nanoparticles (NPs) synthesis. The availability of a large interfacial area of highly stable bridged droplets as a microreactor in comparison to a flat interface provides an efficient platform for interfacial NPs synthesis. To this end, we utilize remarkably stable bridged microreactors, engineered by tuning particle wettability and their adhesion to the interface. The bridged microreactors are created by in situ surface modification of calcium carbonate particles in the water-dodecane system. Then, silica NPs are synthesized by hydrolysis of tetraethyl orthosilicate (TEOS, in the oil phase) at the interface of microreactors in the presence of ammonia catalyst in the aqueous phase. The characterization of the reaction product by XRD, SEM, and TEM confirms the synthesis of silica nanoparticles. This route achieves a complete conversion of TEOS within 2 days, while the flat interface route requires over 15 days. This significant reduction in the reaction time is due to the high oil phase volume to the surface area ratio of spherical droplets and the availability of a large total interfacial area for the reaction. This microreactors route facilitates control over yield and particle size by tailoring reaction time and TEOS concentration. Further, the potential of microreactors route in designing silica hollow microspheres and fluorescent nanoflakes is demonstrated by leveraging the interfacial synthesis at high TEOS concentration. This research

	establishes particle-bridged microreactors as a novel, high-yield, faster-conversion, and versatile pathway for interfacial NPs synthesis. 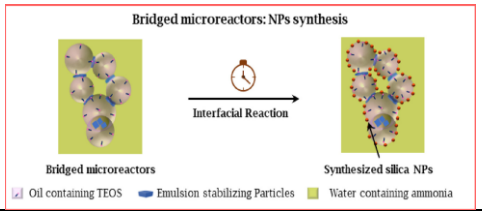
59.	Investigating fission-like fragments in 208Pb (12C, x) 220Ra reaction at E⋆= 39.6 and 45.4 MeV **R Kaur, Amanjot, Priyanka, M Kaushik,** S Kumar…**PP Singh** - Results in Physics, 2025 **Abstract:** The cross-sections of 25 fission-like fragments within the mass range 76≤ A≤ 141, expected to be populated via fission of 220 Ra in 12 C+ 208 Pb system at E lab= 81.9 and 75.8 MeV, have been measured using offline activation analysis. The production yields of different fission-like fragments have been analyzed to generate isotopic and isobaric yield distributions. In the present work, the value of the mass dispersion parameter of fission-like fragments, σ A 2, is found to be 2.93 and 2.65 for Antimony (Sb) at excitation energy E⋆= 45.4 and 39.6 MeV, and 1.24 for Indium (In) isotope at E⋆= 45.4 MeV. The charge dispersion parameter (σ Z) for Sb is estimated to be 0.769 and 0.714 at E⋆= 45.4 and 39.6 MeV, respectively. For In isotopes, the value of σ Z is found to be 0.430 at E⋆= 45.4 MeV. The values of mass and charge dispersion parameters for Sb and In isotopes show good agreement with those reported in the literature for similar systems. Further, the mass distribution of fission-like fragments is found to be fitted with a Gaussian function, except for a few fragments, indicating their production via compound nucleus fission. The mass variance (σ M 2), obtained from the analysis of mass distributions, increases linearly with the compound nucleus excitation energy, indicating the fission-fragments mass spread with the excitation energy.
60.	Investigating the multifunctional coating design for metal surfaces: insights from molecular dynamics simulations **M Moirangthem, K Kumar, L Dhanda, SK Meena** - ACS Omega, 2025 **Abstract:** This study employs molecular dynamics (MD) simulations to evaluate 1*H*,1*H*,2*H*,2*H*-perfluorooctyltriethoxysilane (PFTS) as a multifunctional SAM coating for aluminum surface and compares it with *N*-octyltriethoxysilane (OTES) (same headgroup, no perfluorinated tail) and 1*H*,1*H*,2*H*,2*H*-perfluorooctyltriethoxysilane (PFTCS) (similar tail, different headgroup). DFT calculations suggest that PFTS exhibits a high E_{HOMO} energy level, a small band gap, and very low chemical hardness, positioning it as the most effective inhibitor of corrosion and staining. Complementary MD simulations revealed that the PFTS-SAM has the highest binding energy (−124.68 kJ mol^{-1} per molecule) compared with the OTES-SAM (−90.33 kJ mol^{-1}) and the PFTCS-SAM (−64.54 kJ mol^{-1}), indicating superior surface anchoring and stability. This is due to the synergistic effect of the trialkoxysilane headgroup, which promotes strong adhesion to the aluminum surface, and its robust perfluorinated tail, which enhances intermolecular interactions and contributes hydrophobicity. This dual functionality yields a stable SAM with exceptional anticorrosion and antistain properties. Contact angle analysis confirms the hydrophobic nature of the PFTS-SAM, while thermal stability analyses validate its resilience at elevated temperatures. Additionally, the stress–strain profile illustrates its robustness as a stable coating material. These results position PFTS as a high-performance single-component coating offering multifunctional protection and reduced maintenance, and demonstrate a transferable MD framework for evaluating advanced innovative coatings. 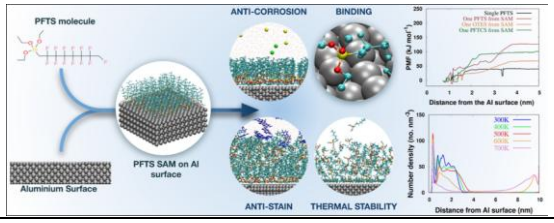

61.	Mechanical performance and predictive tribological modeling of Al7075 composites reinforced with rice hull activated carbon S Banoth, SB Valasingam, R Gujjala, **P Kumar**, S Pratap, P Asaithambi - Scientific Reports, 2025 **Abstract:** This work reports the development of a sustainable Al7075 metal matrix composite reinforced with bio-derived activated carbon (AC) obtained from rice hull agricultural waste. Unlike conventional reinforcements such as SiC and Al_2O_3, rice hull-derived AC provides an eco-friendly, lightweight, and cost-effective alternative. The composites were fabricated using ultrasonic stir casting with varying AC contents (2–8 wt%). Microstructural characterization (OM, FESEM-EDS, and XRD) confirmed uniform dispersion of AC and the absence of detrimental Al_4C_3 formation. Mechanical testing revealed that 2 wt% AC yielded the optimum properties, improving hardness (by 21%) and tensile strength (by 23%) compared to unreinforced Al7075. Abrasive wear studies showed enhanced wear resistance and reduced coefficient of friction at the same reinforcement level. Beyond mechanical and tribological assessment, this work introduces a predictive framework using machine learning models (Gradient Boosted Trees, Gaussian Process Regression), which achieved near-perfect accuracy ($R^2 > 0.99$ for wear, $R^2 > 0.96$ for COF). These findings establish rice hull–derived activated carbon as a viable reinforcement for Al7075 composites and highlight the potential of data-driven approaches in predicting tribological performance, thereby advancing sustainable and intelligent material design.
62.	Microstructure and mechanical property evaluation of A356 alloy casted in conventional silica sand mold and silico-manganese slag blended silica sand mold T Talapaneni… **K Venkatesh** - Transactions of the Indian Institute of Metals, 2025 **Abstract:** The present study evaluates the microstructural and mechanical performance of A356 aluminum alloy castings prepared by two mold compositions: a conventional sand mold and a silica sand mold modified with 15% Silico-Manganese (Si-Mn) slag. The cast products were considered for microstructural analysis, Secondary Dendrite Arm Spacing (SDAS), porosity, surface roughness, and the mechanical behavior was assessed through hardness, tensile strength, and impact toughness. The slag-modified mold (S2) resulted in a refined microstructure, characterized by reduced SDAS (50.86 µm vs. 64.64 µm in conventional S1), finer grains, and more uniform eutectic silicon distribution. While a slight increase in porosity was observed in S2 (2.38%) compared to S1 (0.42%), surface roughness and hardness remained comparable. Mechanical testing revealed enhanced performance in S2 with higher UTS (193.07 MPa), YS (61.44 MPa), elongation (4.17%), and impact toughness (5.24 J), reflecting improved ductility and fracture resistance. XRD analysis confirmed no phase contamination due to slag addition. These findings demonstrate that incorporating 15% Si-Mn slag into sand molds is a promising approach to enhance casting quality and support sustainable waste utilization with minimal environmental impact.
63.	Multifunctional electrospun nanofiber/hydrogel-based pro-healing bilayer dressings as next generation biomaterial for skin wound care D Bhardwaj, **V Chawla**, V Nandwani, **Y Thakur**, **Y Singh**… - Journal of Materials Chemistry B, 2025 **Abstract:** Infectious wounds present a significant challenge in healthcare due to the delay in wound healing and associated processes. Improper use of antibiotics makes this situation even worse due to antibiotic resistance. To meet the critical requirements of healing infectious wounds, we report a bilayer dressing (BL) that combines a hydrogel-based layer and an electrospun nanofiber-based layer together to mimic the dermal and epidermal architecture of normal skin. The bilayer dressing is fabricated by combining a chitosan/gelatin nanofiber-based layer (NF) with an ursodeoxycholic acid drug (UDC) and carbon dot (CD) loaded hydrogel (UDC/CDs/H-Gel). The hydrogel is fabricated by Schiff base-based crosslinking of quaternized chitosan (QCS) and oxidized alginate (OA). The integration of NF with UDC/CDs/H-Gel leads to ~45% increment in tensile strength and ~48% increment in elongation at break. The BL exhibits a swelling of ~400% in 36 h, a porosity of ~75%, and an antioxidant activity of ~93%. Moreover, as compared to individual NF and hydrogel layers, the BL shows good reactive oxygen species (ROS) scavenging behavior, good hemocompatibility (~4.5% hemolysis), good hemostatic potential, enhanced cell proliferation ability (130% cell viability

	of L929 cells), and excellent antibacterial activity with 92% and 88% bactericidal efficacy against E. coli and S. aureus, respectively. The wound healing ability of the BL is further evaluated via scratch assay demonstrating ~97% wound closure. Overall, the BL possesses multifunctionality and presents itself as a potential candidate for accelerated wound healing.
64.	Mycobacterium tuberculosis ACRL protein mitigates experimental autoimmune encephalomyelitis symptoms by generating myeloid-derived suppressor cells and regulatory T cells **T Lamba**, **MA Zafar**, M Shaaz…**MA Khan**, **S Prajapati**, **JA Malik**, **S Nanda**…**JN Agrewala** - Immunology, 2025 **Abstract:** Mycobacterium tuberculosis (Mtb) effectively suppresses host immunity to ensure its survival. We have earlier shown that the Acr1 protein of Mtb can inhibit the differentiation of dendritic cells (DCs). Consequently, in the current study, we examined the role of Acr1 in mitigating autoimmunity. Initially, we observed that Acr1 skews the differentiation of DCs into functionally competent myeloid-derived suppressor cells ($MDSC^{Acr1}$) that chiefly secrete immunosuppressive molecules, expand regulatory T cells ($Treg^{Acr1}$) and attenuate inflammatory responses. Further, $MDSC^{Acr1}$ suppress Th17 cells. Acr1 expanded MDSCs with a concurrent increase in myelin oligodendrocyte glycoprotein (MOG)-specific Tregs and a decline in Th17 cells in a murine experimental autoimmune encephalomyelitis (EAE) model and prevented the onset of the disease. These results were further validated in the prophylactic model of EAE. Mechanistically, Acr1 activates Tregs and MDSCs via the TLR-4 pathway, implicating innate immune recognition in Mtb-induced suppression. The results indicate a potential role of Acr1 against autoimmune diseases.
65.	NSH76: A selective inhibitor of RRN3 and RNA polymerase I transcription with potential for cancer therapy **SS Sarkar**, **M Sharma**, **A Karmakar**, K Jahan…**S Naidu** - Journal of Translational Medicine, 2025 **Abstract: Background:** Aberrant upregulation of RNA polymerase I (Pol I) transcription and its dedicated machinery plays a pivotal role in tumor progression and chemoresistance. RRN3, a Pol I-specific transcription initiation factor, is frequently overexpressed in malignancies contributing to oncogenic processes. Despite the therapeutic potential of Pol I transcription inhibition, existing inhibitors lack specificity and are associated with DNA damage, mutagenicity, and toxicity, limiting their clinical utility. To fully realize the potential of Pol I-targeted cancer therapies, selective Pol I transcription inhibitors with minimal off-target effects are essential. **Methods:** Molecular docking and virtual screening were conducted to identify ligands targeting RRN3. Biochemical and spectroscopic analyses validated the direct ligand-RRN3 binding. The mechanism of action of the ligand was investigated through biochemical, cellular and molecular assays. Functional studies assessed the effects of the ligand on cancer cell viability, clonogenicity, cell cycle progression, and apoptosis, in comparison to non-cancerous cells. The ligand efficacy was further evaluated in chemoresistant cancer cell lines and 3D tumor spheroid models. Genotoxicity and mutagenicity were assessed using DNA damage and mutagenicity assays. **Results:** We demonstrate that (N-(1-amidino-2-thiourea-alkyl-7-chloroquinoline-4-amine)) (NSH76) selectively inhibits Pol I transcription by disrupting the Pol I pre-initiation complex at the rDNA promoter through direct RRN3 binding. Notably, NSH76 does not affect cMyc expression, a Pol II-driven transcript, confirming its specificity. NSH76 preferentially inhibits Pol I transcription in cancer cells with high RRN3 expression, while sparing non-cancerous cells with low RRN3 levels. Functionally, NSH76 exhibits potent antiproliferative activity against cancer cells, with minimal impact on non-cancerous cells. NSH76 induces cell cycle arrest, suppresses clonogenicity, and significantly enhances apoptosis in cancer cells, including cisplatin- and doxorubicin-resistant cell lines. These effects are recapitulated in 3D tumor spheroid assays. Furthermore, NSH76 triggers nucleolar stress, leading to the activation of tumor suppressors p53 and p21. Notably, NSH76 does not induce DNA damage or mutagenicity. **Conclusion:** These findings establish NSH76 as a potent and selective Pol I inhibitor with significant therapeutic potential in cancer and possible implications for overcoming chemoresistance.

	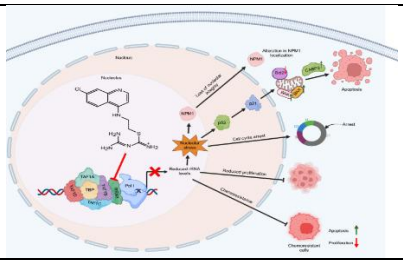
66.	Photocatalytic approach towards benzimidazole synthesis and oxidation of indoles by porphyrins A Janaagal, A Jain, P Maru, **P Chahal, TJD Kumar**, I Gupta - Chemistry-An Asian Journal, 2025 **Abstract:** This work is focused on the photocatalytic applications of three porphyrins having electron-withdrawing and electron-donating groups at their meso-positions. Porphyrins were tested for the diamine coupling reaction and chemoselective oxidation of indole derivatives under visible light. The porphyrin with meso-tetrakis-p-cyanophenyl groups found to be the best photoredox catalyst as compared to the rest of them. For diamine coupling, the method utilizes 0.25 mol% of the porphyrin catalyst and wide variety of aldehydes and diamine were converted to benzimidazole derivatives in high yields (up to 99%). Computational studies were done to optimize the geometry of porphyrin catalysts and provide mechanistic support for the benzimidazole synthesis. Also, oxidation of indole derivatives was achieved in decent to high yields (up to 90%) with just 0.1 mol% of porphyrin, demonstrating the traits of an efficient, and versatile photocatalyst for organic transformations.
67.	Psychological dynamics of terrorism: Insights from individuals exposed to extremist activities embedded in conflict-prone environments **NK Soni, P Singh** - Terrorism and Political Violence, 2025 **Abstract:** Much of the existing research on terrorism relies on third person perspectives or secondary, country-level data, thereby overlooking micro-level psychosocial factors that drive individual radicalization. This study examines the association between cognitive mindset variables—operationalized as self-concept, self-esteem, self-efficacy, empathy, anger, neuroticism, perceived injustice, and social exclusion—and pro-violence proclivity within a terrorism context. For this cross-sectional study, data were collected through self-report instruments and survey questionnaires, targeting two distinct groups of individuals who are above 18 years and belong to Jammu & Kashmir state of India: incarcerated individuals formally charged and under trial for militant behaviour (n = 354) and mainstream youth (n = 516). Statistical analyses, including correlation, regression and t-tests were employed to test the hypotheses. Findings support the hypothesized associations and group differences. The studied factors explained 86 percent of the variance in pro-violence proclivity. Moreover, significant differences were observed between the two groups across all nine attributes, reinforcing the discriminative capacity of the measured constructs. Based on the findings, we propose a PEACE profile—comprising Perceived injustice, Exclusion, Anger, Cognitive mindset (self-concept, self-esteem, self-efficacy, neuroticism), and Empathy—as a critical building block for understanding the social-psychological aspects of terrorism. We argue that managing PEACE factors within a given social setting is likely to emerge as an effective counter terrorism strategy.
68.	Quantification of sub-surface capillary pressure distribution within unstructured superhydrophobic surfaces **K Kamaluddin**, P Dhar, **CS Sharma**, **D Samanta** - Colloids and Surfaces A: Physicochemical and Engineering Aspects, 2025 **Abstract:** We propose a novel methodology for obtaining the sub-surface capillary pressure (Pc) distribution of unstructured superhydrophobic surfaces (USHS), enabling the quantification of its resistance to Cassie to Wenzel transition (CWT) before any direct testing. The method effectively characterizes USHS with completely random textures utilizing surface texture measurements from profilometry. This approach supersedes the standard practice of using a singular Pc value to characterize such surface microtextures, which is often insufficient to capture the uncertainty associated with the wetting transition in the case of USHS. The proposed method incorporates a resolution adequacy check, thereby making the methodology self-regulating and

	ensuring the credibility of the raw profilometer data. We propose a morphological approach using FE-SEM images to obtain reasonable Pc estimates in case obtaining high-resolution profilometry data is not possible. We demonstrated that RSm (mean spacing of profile irregularities) values obtained from the profilometry of USHS help estimate their Pc distribution, offering a scalable route for characterizing USHS. The methodology is validated using elastic non-Newtonian droplets in impact tests on four different types of USHS, showing accurate predictions of Pc distribution. This work addresses a long-standing methodological gap in the characterization of USHS, providing a predictive means to estimate capillary pressure *a priori* to experimental testing. Furthermore, we demonstrate how reliability analysis can be implemented to quantify uncertainty associated with USHS. 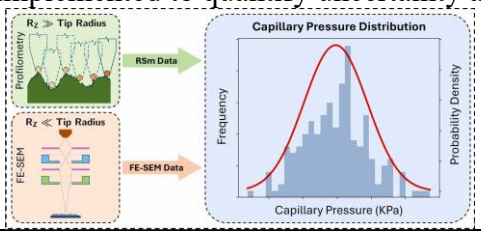
69.	Quantum scattering study of $NCCNH^+$-H_2 collision under interstellar conditions **A Kushwaha, P Chahal, TJ Dhilip Kumar** - Journal of Computational Chemistry, 2025 **Abstract:** The rotational dynamics of protonated cyanogen ($NCCNH^+$) is studied for collision with both para (p-) and ortho (o-) hydrogen (H_2) in the temperature range 1−100 K. Such cold collisions with H_2 are essential to get state-to-state rate coefficients for rotational transitions of newly detected $NCCNH^+$. First, the ab initio 4D potential energy surface (PES) for $NCCNH^+$-H_2 collision is generated at CCSD(T)-F12b level of theory using augmented triple zeta basis, considering rigid rotor approximation. The 4D PES is further fitted into a neural network (NN) model to augment the PES by ∼130 folds. The PES is then expanded using bispherical harmonics functions to get radial terms, which are expressed as analytic functions. The cross-sections and rate coefficients for $NCCNH^+$ are calculated using the exact close-coupling method for rotational states up to j=16 , considering both p- and o-H_2 collisions. The rates show similar behavior to the earlier studied NCCN-H_2 collision, with the latter having larger rate coefficients.
70.	Reductive annealing assisted enhanced oxygen vacancies in MgGa2O4 spinel towards Improved OER and HER electrocatalysis RT Parayil, S Jangra, SK Gupta, **K Garg**… **TC Nagaiah** - Sustainable Energy & Fuels, 2025 **Abstract:** This study explores the synthesis and electrochemical performance of $MgGa_2O_4$-based catalysts which were synthesized under different atmospheric conditions as potential electrocatalysts for the hydrogen evolution reaction (HER) and oxygen evolution reaction (OER). X-ray powder diffraction (XRD) confirmed the phase purity and spinel structure of the synthesized material, with magnesium occupying tetrahedral sites and gallium at octahedral sites, exhibiting partial inverse spinel characteristics. Fourier-transform infrared (FTIR) and Raman spectra further supported the material's structural features. Positron annihilation lifetime spectroscopy (PALS) revealed the presence of significant oxygen vacancies in the sample which was annealed at a reducing atmosphere (MGO-R), enhancing the electrochemical activity. X-ray photoelectron spectroscopy (XPS) analysis showed a higher proportion of oxygen vacancies in MGO-R, corroborating the PALS results. Electrochemical evaluations in 1 M KOH demonstrated that MGO-R outperforms air-annealed $MgGa_2O_4$ (MGO-A) in both the HER and OER, exhibiting superior catalytic activity with lower overpotentials and faster kinetics. MGO-R achieved a hydrogen production current density of 380 mA cm^{-2} at −0.8 V vs. RHE and exhibited a high faradaic efficiency of 98%. Additionally, MGO-R showed excellent OER performance, with a low onset potential of 1.62 V vs. RHE and a faradaic efficiency of 87%. Stability tests confirmed the durability of MGO-R, with minimal degradation over 200 cycles. These results highlight MGO-R's promising potential as an efficient and stable bifunctional electrocatalyst for overall water electrolysis. This work lays the foundation for further development of highly active and durable electrocatalysts for sustainable energy conversion.
71.	Revolutionizing NDT 4.0 with deep attention learning for anomaly detection (DAL-AD) in Mg-based L-PBF components **A Pratap**, **N Sardana**, T Wu… - NDT & E International, 2025

	Abstract: Detection of anomalies in 3D-printed magnesium alloy while printing is difficult because of the reactive nature of the material. In alignment with the principles of Non-Destructive Testing (NDT) 4.0, which emphasizes the inspection of advanced manufacturing processes and fully automated systems, this work presents a novel approach for anomaly detection in additively manufactured parts. Three Mg-based alloy cubes were printed through Selective Laser Melting (SLM) at different scan rates, and X-ray Computed Tomography (XCT) scan was employed to generate the image slices of all three samples. The novel data from all three samples has been selected to segment the anomaly from the printed part. The work has incorporated an innovative approach of adding a saliency map to the model for segmenting the different 3D printed volumes. Incorporating attention layers into the U-net algorithm enhances the learning characteristics of the model by emphasizing the specific region concerning the saliency map. It was found that by using an attention layer in the model, the accuracy in the segmentation of anomalies has been increased compared to simple U-net and other transfer learning approaches as a backbone. The proposed methodology with salient connection has achieved the Dice similarity coefficient (DSC) and Intersection over union (IOU) of 98.29% and 96.67% respectively, demonstrating its effectiveness in the context of NDT 4.0 for the inspection of additively manufactured components. Further aligning the proposed DAL-AD (Deep Attention Learning for Anomaly Detection) framework with broader industrial segments such as Industry 5.0 and ISO 9000, this work enables AI-assisted, sustainable, and in-situ quality control in additive manufacturing.
72.	Risk reduced sparse index tracking portfolio: A topological data analysis approach A Goel, P Pasricha, **J Kanniainen** - Omega, 2025 **Abstract:** In this research, we introduce a novel methodology for the index tracking problem with sparse portfolios by leveraging topological data analysis (TDA). Utilizing persistence homology to measure the riskiness of assets, we introduce a topological method for data-driven learning of the parameters for regularization terms. Specifically, the Vietoris–Rips filtration method is utilized to capture the intricate topological features of asset movements, providing a robust framework for portfolio tracking. Our approach has the advantage of accommodating both l1 and l2 penalty terms without the requirement for expensive estimation procedures. We empirically validate the performance of our methodology against state-of-the-art sparse index tracking techniques, such as Elastic-Net and SLOPE, using a dataset that covers 23 years of S&P 500 index and its constituent data. Our out-of-sample results show that this computationally efficient technique surpasses conventional methods across risk metrics, risk-adjusted performance, and trading expenses in varied market conditions. Furthermore, in turbulent markets, it not only maintains but also enhances tracking performance.
73.	Role of 2D materials in perovskite solar cells B Prajapati, **VK Singh** - Perovskite Solar Cells: Reshaping the Future Energy Landscape, 2025 **Abstract:** Solar photovoltaics, particularly organic/inorganic halide-based perovskite solar cells (PSCs) with high efficiency and cost-effective solution processing, have shown immense potential in harnessing renewable energy to various cause and sustainable economy in recent decades. Though the power conversion efficiency (PCE) of existing PSCs geared up to 26.7% steadily with some fraction of improved stability to earlier ones, there are still some untraceable challenges regarding the upscaling and stability of these promising perovskite-based solar cells. The present chapter highlights the recent developments in PSCs to their peer fabrication, performance, and commercialization. In addition, the chapter also provides in-depth knowledge of various factors affecting solar cell efficiency with possible remedies such as by using two-dimensional (2D) materials as electrodes, additives, and charge transport layers to overcome them. Therefore, this chapter will be helpful to understand the importance of 2D materials, particularly electrode materials and additives, and the existing charge (electron–hole) transport to enhance the power conversion efficiency of perovskite with relatively improved stability of solar cells from laboratory to commercial applications.

74.	Scattering of water waves by multiple porous plates with variable porosity over an undulated bottom **N Sharma**, **SC Martha**, CC Tsai - Physics of Fluids, 2025 **Abstract:** The water wave interaction with multiple floating thin porous plates with varying porosity placed over an undulating seabed is investigated using linear potential flow theory. The porous plate is modeled based on ["Wave transmission through permeable breakwaters," Sollitt and Cross Coastal Eng. 1827–1846 (1972)] theory. The undulated bottom is approximated through stepwise discretization, representing it as a sequence of steps and shelves. The model includes several plate configurations governed by a set of indices, each corresponding to a region containing a porous plate. Further, the porosity variation is incorporated through a piecewise-constant approximation. The problem is formulated assuming the fluid is incompressible and inviscid. By using the method of step approximation and the eigenfunction expansion method, the problem coins to a system of equations, which is solved numerically to compute the values of reflection, transmission coefficients, energy dissipation, and free surface elevation. The model is validated against existing results and through the energy balance relation. The effects of plate arrangements with or without a gap, wave incidence angle, seabed undulation parameters, and different variable porosity patterns (increasing, sinusoidal, constant, and decreasing) are examined. The influence of varying porosity patterns on wave characteristics indicates that a decreasing porosity pattern provides 5% more energy dissipation as compared to a constant porosity pattern. Further comparison among the three types of decreasing porosity configurations highlights their effectiveness, revealing that the quadratic decreasing pattern results in greater dissipation and reduced reflection. Additionally, the study investigates porous plates with intervening gaps, demonstrating that placing the plates with gaps can result in higher dissipation, but only up to a certain gap size. Also, the effect of the optimal number of plates and the placement of plates is also analyzed.
75.	Synergistic effects of interlayer anions in NiFe-LDH and nickel cobaltite heterointerface for energy-efficient alkaline water electrolysis M Sharma, C Prakash, **VK Singh**, A Dixit - ACS Applied Materials & Interfaces, 2025 **Abstract:** An energy-efficient, economically viable, and catalytically active bifunctional electrocatalyst with long-term stability could be a promising alternative to existing noble-metal-based electrocatalysts for producing carbon-neutral green hydrogen via alkaline water electrolysis (AWE). Here, we designed a nanostructured electrocatalyst, i.e., NiFe-LDH electrodeposited on hydrothermally grown Nickel Cobaltite (NCO) over a carbon cloth (CC) substrate, specified as NiFe-LDH/NCO@CC. A phase-pure synthesis is verified by an X-ray diffraction study, and field emission scanning electron microscopy suggests a core–shell (NiFe-LDH/NCO@CC) heterointerface composed of a core of NCO nanowires decorated with a shell of NiFe-LDH nanosheets for sulfate-anion intercalation and NiFe-LDH nanoparticles for nitrate-anion intercalation. The electrochemical analysis performed in 1 M KOH suggests that the optimized sulfate-intercalated NiFe-LDH/NCO@CC electrocatalyst shows superior electrochemical activity compared to pristine NiFe-LDH, NCO, and bare CC, with an overpotential η_{10} of ∼141 and 226 mV for HER and OER, respectively. This superior performance is attributed to the heterointerface of anion-intercalated NiFe-LDH and NCO, which synergistically regulate the electronic structure, facilitating efficient charge transfer at the electrode–electrolyte interface. It can act as a bifunctional catalyst with an overall cell potential of ∼1.66 V, delivering a current density of 10 mA cm^{-2}. It shows a high turnover frequency (TOF) of 5.64×10^{-2} H_2 s^{-1} and 3.75×10^{-2} O_2 s^{-1} at an overpotential of 260 mV. An anion-exchange membrane-based alkaline water electrolyzer is also tested with the synthesized electrocatalyst, showing prolonged stability of ∼50 h in an alkaline medium. The estimation of H_2 production cost reveals that NFS/NCO24@CC requires $1.28/gasoline-gallon equivalent of H_2, which is less than the targeted cost set by the US Department of Energy for 2026. Thus, the present findings reveal that this heterostructure can be a feasible and cost-effective bifunctional electrocatalyst for energy-efficient overall water splitting.

	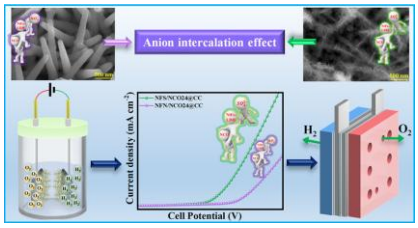
76.	Terahertz multiband notch filter based on a dielectric topological valley photonic crystal R KM, B Mohanta, SM Tripathi, PK Sarswat, **G Kumar** - Journal of Applied Physics, 2025 **Abstract:** This study presents the design of a terahertz multiband notch filter based on a dielectric topological valley photonic crystal (VPC) using a cavity-integrated Mach-Zehnder interferometer geometry. The filter exploits valley-protected edge states created via inversion symmetry breaking in a 2D dielectric-air VPC structure, resulting in a bandgap spanning 310-340 GHz. By integrating a triangular resonator within the VPC, the number of stopbands increased from 1 to 4, considering a reference attenuation depth of −3 dB. The attenuation depth significantly improved from −1.2 to −3.29 dB at 312.7 GHz and from −0.4 to −13.09 dB at 330.6 GHz. The maximum depth of attenuation achieved is −18.51 dB at 327.7 GHz, with a very sharp attenuation profile. Rigorous simulations reveal that the formation and enhancement of the notches arise from the coupling of eigenmodes. Additionally, the impact of the resonator's position on filtering characteristics is quantitatively analyzed, showing that increased cavity distance reduces coupling strength and diminishes filtering performance. The proposed VPC-based filter could be crucial in compact, high-performance THz photonic applications in 6G and beyond communication and sensing technologies.
77.	The role of activity in the nonlinear rheology and flow processes of active fiber (Turbatrix aceti) suspensions **N Ali, M Mishra, V Mehandia** - Physics of Fluids, 2025 **Abstract:** Nematodes, with their active motility and fiber-like structure, serve as excellent models for studying active fluid behavior. This study explores the nonlinear rheology of active and inactive Turbatrix aceti suspensions using large amplitude oscillatory shear experiments and applying the sequence of physical processes method to assess Cole-Cole plots and Trefoil profiles in addition to storage and loss moduli (G' and G'') and loss factor [$\tan(\delta)$] to explore the interplay between activity-induced and externally applied flow effects. At low frequencies, active suspensions display a stable viscoelastic state [($G' \approx G''$)] without crossover, transitioning to a viscous regime at higher strain amplitudes. Inactive/passive suspensions, in contrast, exhibit viscoelastic gel-like behavior ($G' > G''$) with clear crossover points. The transition points shift to lower strains at higher frequencies for both active and passive suspensions. At $f = 4$ Hz , which matches with the nematode's natural undulation frequency (4-6 Hz), active and passive suspensions display similar viscous behavior, indicating that the influence of nematode activity is effectively suppressed by the external flow field. Our study shows that higher frequencies reduce the applied shear strain threshold required to overcome nematode-driven activity, with external power dominating at $f = 4$ Hz . These findings advances our understanding of activity-flow interactions in complex fluids and lays the groundwork for practical applications, such as the design of nematode-inspired microrobots, microfluidic mixers, and design of on-demand flow generating systems for medical and industrial applications.

78.	Thermo-mechanical activation of recycled concrete powders for improved CO2 uptake and mineral stability **P Kalyanasundaram, AS Rajput** - Journal of Building Engineering, 2025 **Abstract:** This study investigates the carbonation potential of Recycled Concrete Powders derived from construction and demolition waste, focusing on the effects of particle size and beneficiation methods. RCP was subjected to mechanical and thermo-mechanical treatments, and then categorized into two size fractions: <150 μm and <300 μm. The influence of these parameters on CO_2 uptake and mineralogical transformation was assessed using a comprehensive suite of characterization techniques, including particle size distribution, X-ray fluorescence, X-ray diffraction, Fourier-transform infrared spectroscopy, Raman spectroscopy, and thermogravimetric analysis. Results showed that thermo-mechanical treatment significantly enhanced carbonation reactivity, with the TM150 fraction achieving the highest CO_2 uptake (9.83 %) and a degree of carbonation of 45.62 % after 24 h of accelerated CO_2 curing. Thermal activation increased oxide availability (notably CaO), while finer particles improved surface reactivity and carbonation kinetics. Spectroscopic and thermal analyses confirmed the conversion of portlandite and C-S-H into stable $CaCO_3$ polymorphs, particularly calcite. This study demonstrates that integrating thermal pre-treatment with particle size refinement offers a promising route for valorizing Recycled Concrete Powders as low-carbon supplementary cementitious materials, contributing to circular construction and carbon sequestration efforts.
79.	TransWaveNet: Transformer for underwater image restoration with wavelets **P Mishra**, MDR Khan…**SK Vipparthi**, S Murala - IEEE Transactions on Artificial Intelligence, 2025 **Abstract:** Underwater image restoration aims to improve the quality and visibility of images taken in underwater environments. These images find application in diverse fields like marine biology research, underwater archaeology, environmental monitoring, surveillance tasks, and offshore infrastructure inspection. However, the complexities of the underwater environment make these applications challenging, as light scattering and absorption cause blur, color cast, and reduced contrast in images. With the promising results on restoring underwater degraded images, existing approaches limit their performance in case of the above-mentioned complex and nonlinear degradation. In this research work, we propose a multi-directional wavelet coefficient space transformer model for underwater image deblurring and color restoration. Incorporating an attention mechanism within transformed spaces, our model dynamically adapts to underwater degradation. Additionally, we introduce a wavelet attention fusion transformer block for attention computation in the wavelet coefficient space, along with an edge-preserving wavelet downsampling block to retain fine details and textures during downsampling. A thorough assessment of our method on real-world (UCCS, U45, SQUID) and synthetic (UIEB, UCDD) datasets, along with profound ablation studies, validates its edge over existing techniques. Further, we have evaluated our method for tasks such as depth estimation, and low-light enhancement and deblurring, demonstrating its versatility and broad applicability across various image processing tasks.
80.	Tribological, mechanical, and cytocompatibility characteristics to study surface integrity of titanium–hydroxyapatite sintered bio-composites for implant applications **R Kumar, A Agrawal** - Journal of Materials Engineering and Performance, 2025 **Abstract:** Metallic implants have been widely used for their structural rigidity, mechanical strength, and long lifespan as a replacement for load-bearing bones. However, the primary concern with metal-based implants is stress-shielding and implant-tissue interface caused by large variations in mechanical properties of the used implant material and tissue interface, affecting the performance of actual body functions by deteriorating surrounding natural bones and tissues. The present work attempts to characterize microwave sintered Ti-μ-HAp bio-composite with various compositions having enhanced stress-shielding effect and interface properties through their tribological characteristics using nano-mechanical, surface-wear, wettability, and corrosion tests. In vitro bio-compatibility tests with mouse fibroblast cells have been performed to analyze cell adhesion and growth. Detailed microscopy and elemental distribution characterizations have been studied to exhibit

	the diffusion of HAp in the composite. An appreciable reduction in modulus, nano-hardness, and coefficient of friction with increasing HAp composition exhibits desired tailored properties for load-bearing implant applications. A comprehensive study confirms enhanced bioactivity (− 50% increased cell absorbance for 3 wt.% HAp composite compared to commercially Pure Ti), considerable corrosion rate with apatite formation, and tribological properties for the proposed metal–ceramic-composites, which could be a better substitute for metallic biomaterials for hard tissue applications. 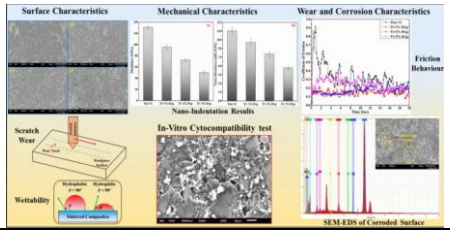
81.	Unveiling the evolution of microstructural and optoelectronic properties of spray-pyrolyzed ZnO thin films via tailoring the aerosol deposition time CM Mahajan, **SP Gumfekar** - The Canadian Journal of Chemical Engineering, 2025 **Abstract:** ZnO thin films with diverse thicknesses were deposited via the spray pyrolysis technique by varying the deposition time (τ). The XRD analysis shows an increase in polycrystallinity for films with an increase in τ; however, all films exhibit predominant growth along the c-axis [002] direction. The FE-SEM analysis shows the growth of well-aligned ZnO nanorods upright on the substrate at τ = 20 min. EDS analysis confirms the high quality ZnO film formation with a slightly rich oxygen concentration. The films exhibit optical transmittance >90%, with the highest of 95% when deposited for 24 min. There is a rise in crystallite size along with film thickness; however, bandgap energy (E_g) declines with a rise in τ. The inverse relation of E_g with Urbach energy (E_u) is attributed to superior crystallinity at lower E_u. Under optimal deposition time τ = 20 min, the film shows the highest dark conductivity 108.2 S/cm, free electron concentration $\eta = 3.76 \times 10^{19}$ /cm^3, and mobility $\mu = 17.98$ cm^{2}V^{-1} s^{-1}. For τ = 20 min, the film exhibits the best figure of merit, $\Phi_{TC\text{-}H} = 2.03 \times 10^{-3}\ \Omega^{-1}$, $\Phi_{TC\text{-}H\text{-}HR} = 4.11 \times 10^{-2}\ \Omega^{-1/12}$, and the least sheet resistance, $R_s = 275\ \Omega/\square$. © 2025 Canadian Society for Chemical Engineering.

Disclaimer: This publication digest may not contain all the papers published. Library has compiled the publication data as per the alerts received from Scopus and Google Scholar for the affiliation “Indian Institute of Technology Ropar” for the month of October, 2025. The author(s) are requested to share their missing paper(s) details if any, for the inclusion in the next publication digest.